

AD-A113 007

ROCKWELL INTERNATIONAL THOUSAND OAKS CA MICROELECTR--ETC F/G 20/12

GAAS SURFACE PASSIVATION FOR DEVICE APPLICATIONS.(U)

DEC 81 R W GRANT, K R ELLIOTT, S P KOWALCZYK F33615-78-C-1591

UNCLASSIFIED

ERC41051.411TR

AFWAL-TR-81-1209

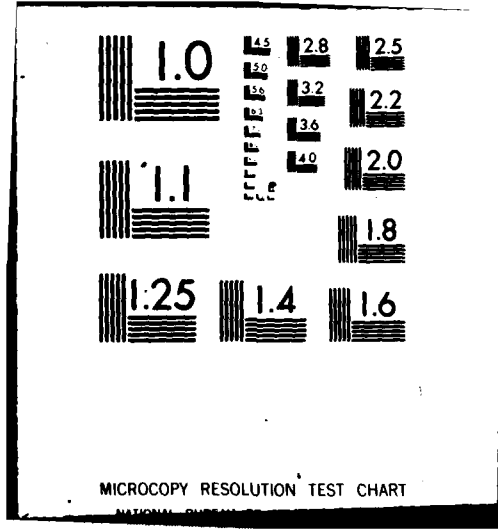
NL

1-1
2-2

■

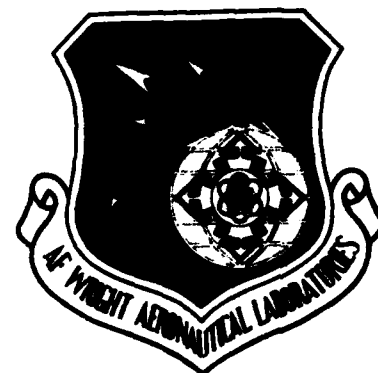
■	■	■	■	■	■	■	■	■	■	■	■	■	■	■
■	■	■	■	■	■	■	■	■	■	■	■	■	■	■
■	■	■	■	■	■	■	■	■	■	■	■	■	■	■
■	■	■	■	■	■	■	■	■	■	■	■	■	■	■
■	■	■	■	■	■	■	■	■	■	■	■	■	■	■

END
DATE
FILMED
4-82
DTIC



12

AFWAL-TR-81-1209



GaAs SURFACE PASSIVATION FOR DEVICE APPLICATIONS

R.W. Grant, K.R. Elliott, S.P. Kowalczyk, D.L. Miller and
J.R. Waldrop

Rockwell International Microelectronics Research and
Development Center
1049 Camino Dos Rios
Thousand Oaks, CA 91360

December 1981

Interim Report for Period 1 April 1980 - 30 September 1980

Approved for public release; distribution unlimited

Aeronics Laboratory
Air Force Wright Aeronautical Laboratories
Air Force Systems Command
Wright-Patterson Air Force Base, Ohio 45433

DTIC
ELECTE
APR 5 1982
B

DTIC FILE COPY

AD A11 8007

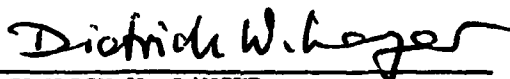
82 04 05 08 9

NOTICE

When Government drawings, specifications, or other data are used for any purpose other than in connection with a definitely related Government procurement operation, the United States Government thereby incurs no responsibility nor any obligation whatsoever; and the fact that the government may have formulated, furnished, or in any way supplied the said drawings, specifications, or other data, is not to be regarded by implication or otherwise as in any manner licensing the holder or any other person or corporation, or conveying any rights or permission to manufacture use, or sell any patented invention that may in any way be related thereto.

This report has been reviewed by the Office of Public Affairs (ASD/PA) and is releasable to the National Technical Information Service (NTIS). At NTIS, it will be available to the general public, including foreign nations.

This technical report has been reviewed and is approved for publication.



DIETRICH W. LANGER
Project Engineer
Electronic Research Branch
Avionics Laboratory

FOR THE COMMANDER



PHILIP E. STOVER, Chief
Electronic Research Branch
Avionics Laboratory

"If your address has changed, if you wish to be removed from our mailing list, or if the addressee is no longer employed by your organization please notify AFWAL/AADR, W-PAFB, OH 45433 to help us maintain a current mailing list."

Copies of this report should not be returned unless return is required by security considerations, contractual obligations, or notice on a specific document.

UNCLASSIFIED

SECURITY CLASSIFICATION OF THIS PAGE (When Data Entered)

REPORT DOCUMENTATION PAGE		READ INSTRUCTIONS BEFORE COMPLETING FORM
1. REPORT NUMBER AFWAL-TR-81-1209	2. GOVT ACCESSION NO. AD-A223 007	3. RECIPIENT'S CATALOG NUMBER
4. TITLE (and Subtitle) GaAs SURFACE PASSIVATION FOR DEVICE APPLICATIONS		5. TYPE OF REPORT & PERIOD COVERED Interim Technical Report for 1 Apr 80 - 30 Sep 80
		6. PERFORMING ORG. REPORT NUMBER ERC41051.41ITR
7. AUTHOR(s) R.W. Grant, K.R. Elliott, S.P. Kowalczyk, D.L. Miller and J.R. Waldrop		8. CONTRACT OR GRANT NUMBER(s) F33615-78-C-1591
9. PERFORMING ORGANIZATION NAME AND ADDRESS Rockwell International Microelectronics Research & Development Center P.O. Box 1085, Thousand Oaks, CA 91360		10. PROGRAM ELEMENT, PROJECT, TASK AREA & WORK UNIT NUMBERS 61102F/2305R/R1/82
11. CONTROLLING OFFICE NAME AND ADDRESS Air Force Avionics Laboratory ATTN: AFWAL/AADR Wright Patterson AFB, OH 45433		12. REPORT DATE December 1981
		13. NUMBER OF PAGES 67
14. MONITORING AGENCY NAME & ADDRESS (if different from Controlling Office)		15. SECURITY CLASS. (of this report) UNCLASSIFIED
		16. DECLASSIFICATION/DOWNGRADING SCHEDULE
16. DISTRIBUTION STATEMENT (of this Report) Approved for public release; distribution unlimited.		
17. DISTRIBUTION STATEMENT (of the abstract entered in Block 20, if different from Report)		
18. SUPPLEMENTARY NOTES		
19. KEY WORDS (Continue on reverse side if necessary and identify by block number) Gallium Arsenide Surface Passivation Oxidation XPS Gallium Aluminum Arsenide MBE Insulation		
20. ABSTRACT (Continue on reverse side if necessary and identify by block number) This document is the Interim Report #4 which covers the period 4/1/80 through 9/30/80 for contract No. F33615-78-C-1591 entitled, "GaAs Surface Passivation for Device Applications." C-V and I-V measurements are reported for several GaAs (100) MIS samples of both n- and p-type. The insulators were formed by thermal oxidation of MBE grown $Al_{1-x}Ga_xAs$ layers or by evaporation of SiO_x . A photochemical process was developed to deposit SiO_2 on room temperature samples.		

DD FORM 1 JAN 79 1473 EDITION OF 1 NOV 65 IS OBSOLETE

UNCLASSIFIED
SECURITY CLASSIFICATION OF THIS PAGE (When Data Entered)

i/ii

TABLE OF CONTENTS

<u>Section</u>	<u>Page</u>
SUMMARY.....	viii
I. INTRODUCTION.....	1
II. SAMPLE PREPARATION.....	3
1. MBE Samples.....	3
2. Deposited Insulators.....	7
3. XPS Study of Aluminum Oxide Growth.....	13
III. SAMPLE ANALYSIS.....	18
1. C-V and I-V Measurements.....	18
a. MBE Samples.....	18
b. Deposited Insulator Samples.....	28
2. Depth Profile of Sample No. 411.....	37
IV. DISCUSSION OF PREVIOUS MBE RESULTS.....	42
REFERENCES.....	46
APPENDIX.....	48

Accession For	
NTIS GRA&I	<input checked="checked" type="checkbox"/>
DTIC TAB	<input type="checkbox"/>
Unannounced	<input type="checkbox"/>
Justification.....	
By.....	
Distribution/	
Availability Codes	
Dist	Avail and/or Special
A	



LIST OF ILLUSTRATIONS

<u>Figure</u>		<u>Page</u>
1	Schematic illustration of structure for three MBE samples.....	4
2	Idealized flat-band diagram constructed assuming that ~ 88% of energy gap discontinuity is associated with the conduction-band edge (E_c) and ~ 12% with the valence band edge (E_v).....	6
3	XPS spectrum of evaporated SiO_x	10
4	XPS spectra in binding-energy region of Si 2p line for (top) SiO_x material before evaporation (middle) SiO_x after vacuum evaporation and (bottom) SiO_x after evaporation in O_2 with presence of UV light.....	11
5	XPS spectra in region of Al 2p line for (A) evaporation of Al in O_2 with UV light present, and (B) oxidation of Al film in (A) at ~ 510°C.....	14
6	XPS spectra in region of Al 2p line for (C) additional Al evaporated in O_2 onto the surface characterized as spectrum (B) in Fig. 5 while this surface was at 520°C and (D) oxidation of sample in (C) at ~ 520°C.....	15
7	XPS spectra in region of Al 2p line. Spectrum labeled (D) is repeated from Fig. 6 for reference. Spectrum (E) was obtained after deposition of Al onto the sample at room temperature while in the presence of an O_2 plasma discharge.....	16
8	C-V measurements for Sample No. 491.....	20
9	C-V measurements for Sample No. 490.....	21
10	C-V measurements for Sample No. 493.....	23
11	C-V measurements at 1 MHz for sample No. 411 after three sequential oxidations, (top) 0.5 min oxidation, (middle) 10 min oxidation, and (bottom) 60 min oxidation.....	24
12	C-V measurements at 1 MHz for same sample as in Fig. 11, (top) 330 min oxidation, (bottom) 1575 min oxidation.....	26
13	C-V measurements at 1 MHz for same sample as in Figs. 11 and 12 after 10,455 min oxidation.....	27

LIST OF ILLUSTRATIONS

<u>Figure</u>		<u>Page</u>
14	C-V measurements at 1 MHz for sample X1.....	29
15	I-V measurements for sample X1 (p-type).....	31
16	Comparison of leakage currents for vacuum evaporated SiO _x and photochemically produced SiO ₂ insulators.....	32
17	C-V measurements at 1 MHz for sample X2 (p-type).....	33
18	C-V measurements at 1 MHz for sample X3 (p-type).....	34
19	C-V measurements at 1 MHz for sample X4 (n-type).....	35
20	C-V measurements at 1 MHz for sample X5 (n-type).....	36
21	C-V measurements at 1 MHz for sample X3 (n-type). Data obtained by B. Bayraktaroglu (WPAFB).....	38
22	G-V measurements at 100 kHz for sample X3 (n-type). Data obtained by B. Bayraktaroglu (WPAFB).....	39
23	Depth profile obtained with SAM for sample #411 after oxidation in O ₂ at 400°C for 10,455 min.....	40
24	C-V measurements for thermally oxidized MBE grown sample of AlAs/graded Al _x Ga _{1-x} As/GaAs replotted from Ref. 1.....	44

LIST OF TABLES

<u>Table</u>		<u>Page</u>
1	Deposited SiO _x experiments.....	9

SUMMARY

$Al_{1-x}Ga_xAs$

Three new MBE grown samples of graded $Al_{1-x}Ga_xAs$ on GaAs (100) have been prepared and characterized in an effort to develop a practical dielectric for GaAs surface passivation. In addition a systematic C-V study of a previously grown MBE structure as a function of oxidation time was carried out. In all cases, the thermal oxide produced on these samples appears to have excessive leakage which may be the cause for the absence of any observed inversion. An analysis of previously published results on thermally oxidized MBE grown graded layers of $Al_{1-x}Ga_xAs$ on GaAs suggests that these results may not be completely understood. Current results suggest that other insulators should be investigated as possible substitutes for the thermally grown oxides.

Several device structures involving deposited SiO_x on GaAs (100) surfaces of known composition did not produce satisfactory C-V results from a passivation criteria. A novel photochemical process was developed to deposit nearly stoichiometric SiO_2 on GaAs surfaces at room temperature. Several methods of depositing Al oxides were investigated; Al deposition in the presence of an O_2 plasma discharge was found to produce relatively thick layers of an intermediate Al oxide.

SECTION I

INTRODUCTION

This is the fourth interim report for Contract No. F33615-78-C-1591 which is entitled "GaAs Surface Passivation for Device Applications." The time period 04/01/80 to 09/30/80 is covered in this report. A goal of this program is to develop a practical dielectric for GaAs surface passivation which would be useful in a GaAs MIS device technology. In December 1979, the program underwent a major redirection. The initial approach which was aimed at developing an amorphous GaPO_4 dielectric by thermal oxidation of a heavily phosphorous implanted GaAs layer was stopped. Since that time two different approaches have been pursued.

The first approach involves attempts to reproduce the promising capacitance-voltage (C-V) results of Tsang et al.¹ In this approach MBE grown structures of graded $\text{Al}_{1-x}\text{Ga}_x\text{As}$ epitaxial layers on GaAs are thermally oxidized to produce a dielectric layer. Results reported in the literature¹ have been interpreted as demonstrating the achievement of inversion and the presence of a low fixed interface state charge density ($<2 \times 10^{10} \text{ cm}^{-2}$).

The second approach utilizes information on interface chemistry and potential obtained by surface analytical techniques in an attempt to control interface properties. After preparation of a GaAs surface with known surface chemistry, a dielectric is deposited to form a MIS structure. C-V and current-voltage (I-V) measurements are the primary means used to characterize the electrical properties of the MIS structures obtained by both approaches.

In Section II of this fourth interim report, the preparation of both the MBE grown samples and deposited insulator samples is discussed. Section III discusses C-V and I-V analyses of the samples and the results of some depth profiles obtained for one of the MBE grown samples. Section IV presents some additional analysis of the previously published¹ C-V results for the thermal oxidation of MBE grown $\text{Al}_{1-x}\text{Ga}_x\text{As}$ layers.

SECTION II

SAMPLE PREPARATION

1. MBE Samples

Three samples were prepared by MBE during this reporting period. All were grown at Thousand Oaks by using our MBE apparatus. The details of the apparatus and growth procedure are as previously reported, except for the changes in sample configuration discussed here. These samples were grown for use in experiments which attempted to duplicate the inversion behavior obtained by using a GaAs-Al_{1-x}Ga_xAs-oxidized AlAs structure as reported by Tsang et al.¹ A diagram of the samples grown is shown in Fig. 1.

All three MBE samples were grown at 620°C substrate temperature, rather than the 580°C used in earlier runs.² This is because data accumulated in a number of laboratories have shown that Al_{1-x}Ga_xAs grown by MBE at 620°C and above is markedly superior to material grown at lower temperatures in terms of carrier mobility, luminescence, and deep-level content. Therefore, it was hoped that Al_{1-x}Ga_xAs grown at this higher substrate temperature would yield better MIS structures than the material used for our previous samples.

A second change was made in using Si, rather than Sn, as the doping for the n-type GaAs buffer layers. This was done to eliminate doping of the Al_{1-x}Ga_xAs graded transition layer due to the well-known Sn surface segregation phenomenon. In MBE growth of GaAs, Sn is incorporated into the growing film from a surface accumulation, which rides along on the growth surface.

MBE SAMPLES

SAMPLE # 490

ALAs	UNDOPED	2000 Å
AL _{1-x} Ga _x As	GRADED	1400 Å
UNDOPED		
GaAs(P)	BE $< 1 \times 10^{16} / \text{cm}^{-3}$	5000 Å
GaAs (P+) SUBSTRATE		

SAMPLE # 491

ALAs	UNDOPED	2000 Å
AL _{1-x} Ga _x As	GRADED	1400 Å
UNDOPED		
GaAs(N)	SI $\approx 1.6 \times 10^{17} / \text{cm}^{-3}$	5000 Å
GaAs (N+) SUBSTRATE		

SAMPLE # 493

ALAs	UNDOPED	2000 Å
AL _{1-x} Ga _x As	GRADED	1400 Å
UNDOPED		
GaAs(P)	BE $\approx 1 \times 10^{17} / \text{cm}^{-3}$	10000 Å
GaAs (P+) SUBSTRATE		

Fig. 1 Schematic illustration of structure for three MBE samples.

This mechanism delays the transient response of the system to changes in dopant flux, and also makes Sn doping sensitive to substrate temperature, alloy composition, and As/Ga flux ratio. Therefore, a Sn-doped sample of the type prepared for these experiments (and also used by Tsang et al)¹ would be expected to have n-type doping extending into the $\text{Al}_{1-x}\text{Ga}_x\text{As}$ graded region. The depth of this unintentional doping will depend on the details of the growth process. The use of Si as a dopant eliminates this effect. Therefore, in these samples, the doping ends abruptly at the $\text{GaAs-Al}_{1-x}\text{Ga}_x\text{As}$ interface.

A third change was to grow samples having a p-type buffer layer. This was done to take advantage of the difference in band discontinuities for the conduction- and valence-bands in the $\text{GaAs-Al}_{1-x}\text{Ga}_x\text{As}$ heterojunction. The band structure for these samples is shown in Fig. 2, for an idealized case which does not show band-bending effects for clarity. The important point of this illustration is that the discontinuity in the conduction band at the $\text{GaAs-Al}_{1-x}\text{Ga}_x\text{As}$ interface is considerably larger than the corresponding discontinuity in the valence band. This diagram assumes that approximately 88% of the bandgap difference falls in the conduction band, with the remaining 12% in the valence band for all $\text{Al}_{1-x}\text{Ga}_x\text{As/GaAs}$ heterojunctions; Dingle et al³ have determined this distribution for a $\text{Al}_{0.2}\text{Ga}_{0.8}\text{As/GaAs}$ heterojunction. Therefore, it may be easier to invert p-type GaAs by confining electrons in the GaAs with the larger (0.33 eV in this case) conduction-band discontinuity than to invert n-type GaAs by confining holes with the smaller (0.05 eV) valence-band discontinuity. This assumes that injection of minority carriers into the $\text{Al}_{1-x}\text{Ga}_x\text{As}$ is largely responsible for a lack of inversion in these structures.

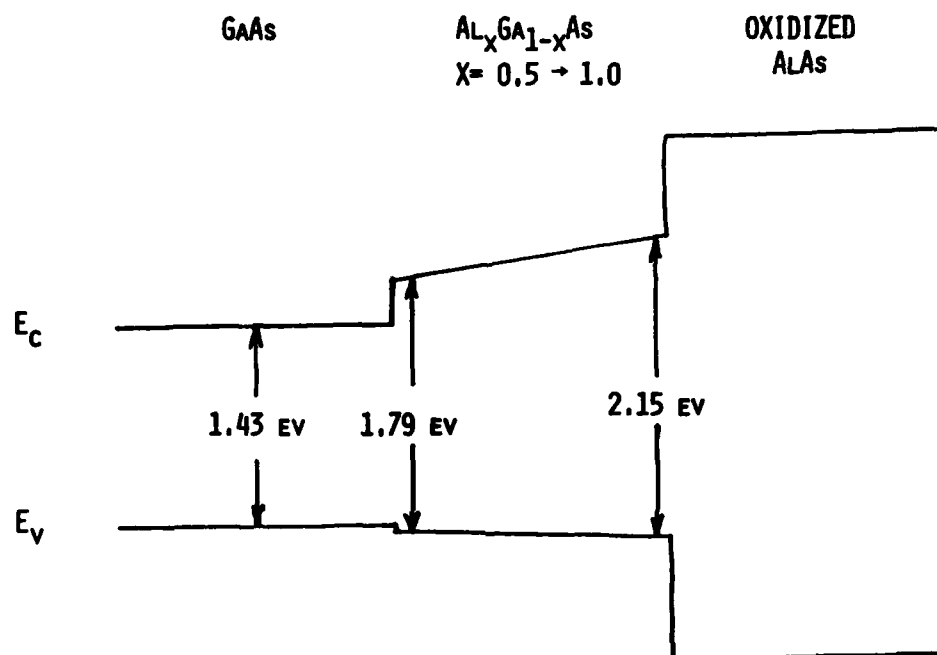


Fig. 2 Idealized flat-band diagram constructed assuming that $\sim 88\%$ of energy gap discontinuity is associated with the conduction-band edge (E_C) and $\sim 12\%$ with the valence band edge (E_V).

The AlAs top layer was oxidized in a separate furnace following growth. The samples were contained in a molybdenum holder which was placed in a quartz tube. The tube was flushed with gaseous O_2 (99.6% purity) for several minutes before inserting into a tube furnace which was maintained at $400 \pm 10^\circ C$. A small flow of O_2 was maintained during the oxidation. These oxidation conditions were chosen to duplicate the work reported in Ref. 1 as nearly as possible.

An additional set of experiments was carried out on a portion of the MBE prepared sample No. 411 (this sample was described in the previous interim report² and had been stored in a vacuum box for ~ 4 months prior to this set of experiments). The sample was oxidized sequentially for increasing lengths of time under the conditions noted in the preceeding paragraph. After each oxidation a row of metal dots was evaporated into the sample surface through a contact mask and C-V data were collected (results are presented in Section III-1-a). The rationale behind this set of experiments was to correlate C-V results with depth of oxidation for a single sample.

2. Deposited Insulators

During this reporting period, ten samples of bulk GaAs (100), which had deposited insulators, were also prepared and investigated. The samples were prepared within the ultra-high vacuum x-ray photoemission spectroscopy (XPS) apparatus which was described in the previous interim report.² Ten samples were prepared in sets of two during five independent experiments. The five sets of samples are identified as X1 through X5. For each preparation,

one $n(= 1 \times 10^{17} \text{ cm}^{-3})$ and one $p(= 2 \times 10^{16} \text{ cm}^{-3})$ sample were prepared. The initial surface treatments were chosen to produce surfaces which had either a few monolayers of Ga_2O_3 present or were clean (prepared by heating the samples to $\sim 560^\circ\text{C}$) as monitored by XPS. Surfaces of these two types are known to have substantially different surface potentials.⁴

The insulator was prepared by evaporating SiO_x onto the sample surfaces within the XPS sample preparation chamber. In most cases the samples were at room temperature, however for sample "X2" the sample was at $\sim 460^\circ\text{C}$. As discussed in the next paragraph, the composition of the insulator, as determined by the Si^{4+} / reduced Si ratio, could be varied substantially by changing the ambient for the SiO_x deposition. In Table 1, the initial surface preparation conditions, the ambient condition during the SiO_x deposition, and the insulator composition as determined by XPS analysis are summarized for samples X1 through X5.

Table 1
Deposited SiO_x Experiments

Sample No.	Surface Preparation	SiO _x Deposition Conditions	Insulator Composition
X1	Thermally Cleaned 6 × 10 ⁴ L O ₂ at ~ 460°C Stored in Vac. 9 hrs.	Vacuum Evaporation Sample at R.T.	Reduced Si Present
X2	Heated to ~ 460°C to Form Ga ₂ O ₃	3 × 10 ⁻⁵ torr O ₂ UV Sample at ~ 460°C	Small but Detectable Amount of Reduced Si
X3	Thermally cleaned 6 × 10 ⁴ L O ₂ at ~ 460°C	3 × 10 ⁻⁵ torr O ₂ UV Sample at R.T.	No Reduced Si Detected
X4	Heated to ~ 460°C to Form Ga ₂ O ₃	3 × 10 ⁻⁵ torr O ₂ UV Sample at R.T.	No Reduced Si Detected
X5	Thermally Cleaned	1 × 10 ⁻⁴ torr O ₂ UV Sample at R.T.	No Reduced Si Detected

During the course of these experiments it was observed by XPS that the composition of the deposited SiO_x could be varied substantially by changing the ambient. In Fig. 3 an XPS spectrum of SiO_x evaporated in vacuum is shown. The figure illustrates the elemental purity of the insulator as only photoelectron lines associated with Si 2p (binding energy ~ 100 eV), Si 2s (~ 150 eV), O 1s (~ 530 eV) and an oxygen Auger line at ~ 980 eV are visible. At the top of Fig. 4 an XPS spectrum in the binding energy region of Si 2p is

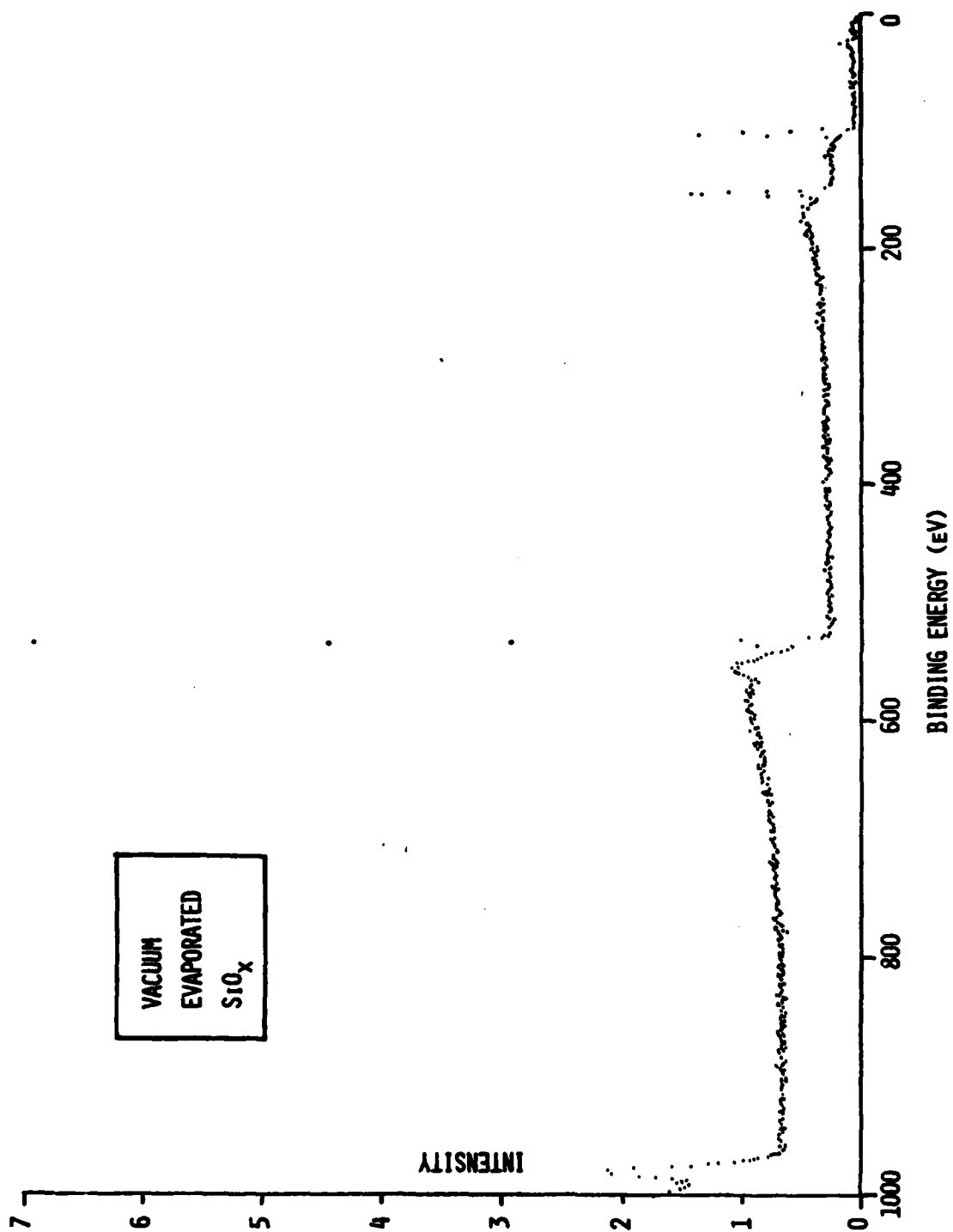


Fig. 3 XPS spectrum of evaporated SiO_x .

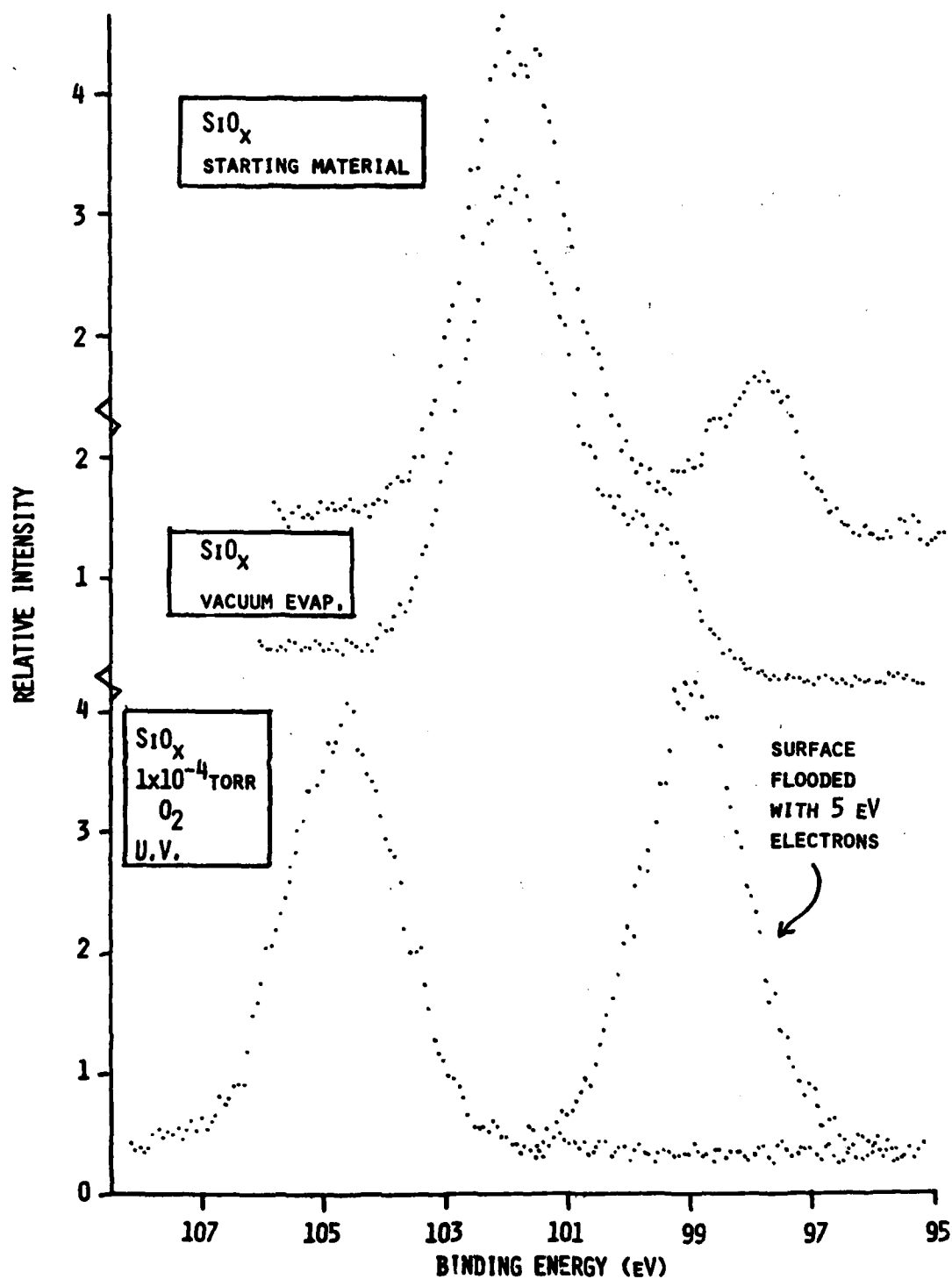


Fig. 4 XPS spectra in binding-energy region of Si 2p line for (top) SiO_x material before evaporation (middle) SiO_x after vacuum evaporation and (bottom) SiO_x after evaporation in O_2 with presence of UV light.

shown for the SiO_x starting material (before evaporation). By using the chemical shift scale of Adachi and Helms,⁵ the major Si 2p peak is identified as Si^{4+} while the less intense peak is associated with Si^0 . Evaporation of this same starting material in vacuum (or in $\sim 10^{-5}$ torr O_2) produces a film which contains reduced Si (spectrum in middle of Fig. 4). From the chemical shift scale of Ref. 5, this reduced form of Si is most likely Si^{2+} . Photochemical reactions can be induced by ultraviolet (UV) excitation (see for e.g., the discussion of Al_2O_3 growth on GaAs by evaporation of Al in O_2 by Yokoyama et al).⁶ This possibility was investigated for the SiO_x deposition. Evaporation of the SiO_x source material with the sample preparation chamber filled to 10^{-4} - 10^{-5} torr of O_2 which was illuminated by UV radiation produced in a film with only one detectable Si oxidation state as indicated by the two XPS spectra shown at the bottom of Fig. 4. This sample charged positively under illumination by the XPS x-ray beam and consequently the relative binding-energy scale cannot be compared directly with the spectra at the top and middle of Fig. 4. The sample charging effect is easily observed by flooding the sample surface with 5 eV electrons and noting the large shift in the apparent Si 2p binding energy (see bottom of Fig. 4). The relative binding energy difference between the Si 2p and O 1s photoelectron peaks indicates that this sample is SiO_2 to within the analysis limits of the XPS technique.

The dielectric properties of the deposited SiO_x improve markedly as the amount of reduced Si is decreased. This observation will be noted further in Section III-1-b.

3. XPS Study of Aluminum Oxide Growth

Thermal oxidation of aluminum usually results in polycrystalline oxide films of poor quality.⁷ We thus initiated a study to investigate the growth of aluminum oxide by other methods with the desire to find a method which would allow growth of Al oxide at room temperature. The preparation methods were compared by using XPS. The initial studies include (A) slow evaporation of Al in O₂ background under UV irradiation (Hg lamp), (B) and (D) heating of film at ~ 510°C under O₂ exposure, (C) deposition of Al during O₂ exposure on a heated substrate, and (E) deposition of Al under conditions of O₂ plasma discharge onto a room temperature substrate. The XPS spectra in the Al 2p region are shown in Figs. 5-7. The Al metal 2p level has a binding energy of ~ 72.6 eV relative to the Fermi level. All spectra in Figs. 5-7 are referenced to Al metal. Figure 5 shows the results for deposition under UV irradiation. This film is mostly Al metal but also has at least two different oxides with chemical shifts of ~ 3.0 and ~ 2.0 eV, the former being similar to the characteristic ~ 2.8 eV shift of bulk Al₂O₃ and the latter being some intermediate form of oxide. A slower deposition rate could possibly yield a film that is totally oxide. Heating this film to ~ 510°C in 5×10^{-5} torr O₂ almost totally converts this film to the intermediate oxide. Another film investigated was one prepared by Al deposition in 1×10^{-4} torr O₂ onto a substrate at ~ 520°C. This preparation leads to a mixture of Al metal and Al oxide with the ~ 3.0 eV chemical shift and is thus similar to bulk oxide. Again the deposition rate was probably too fast for total oxidation. Further heating this film converts the film almost totally to aluminum oxide. The

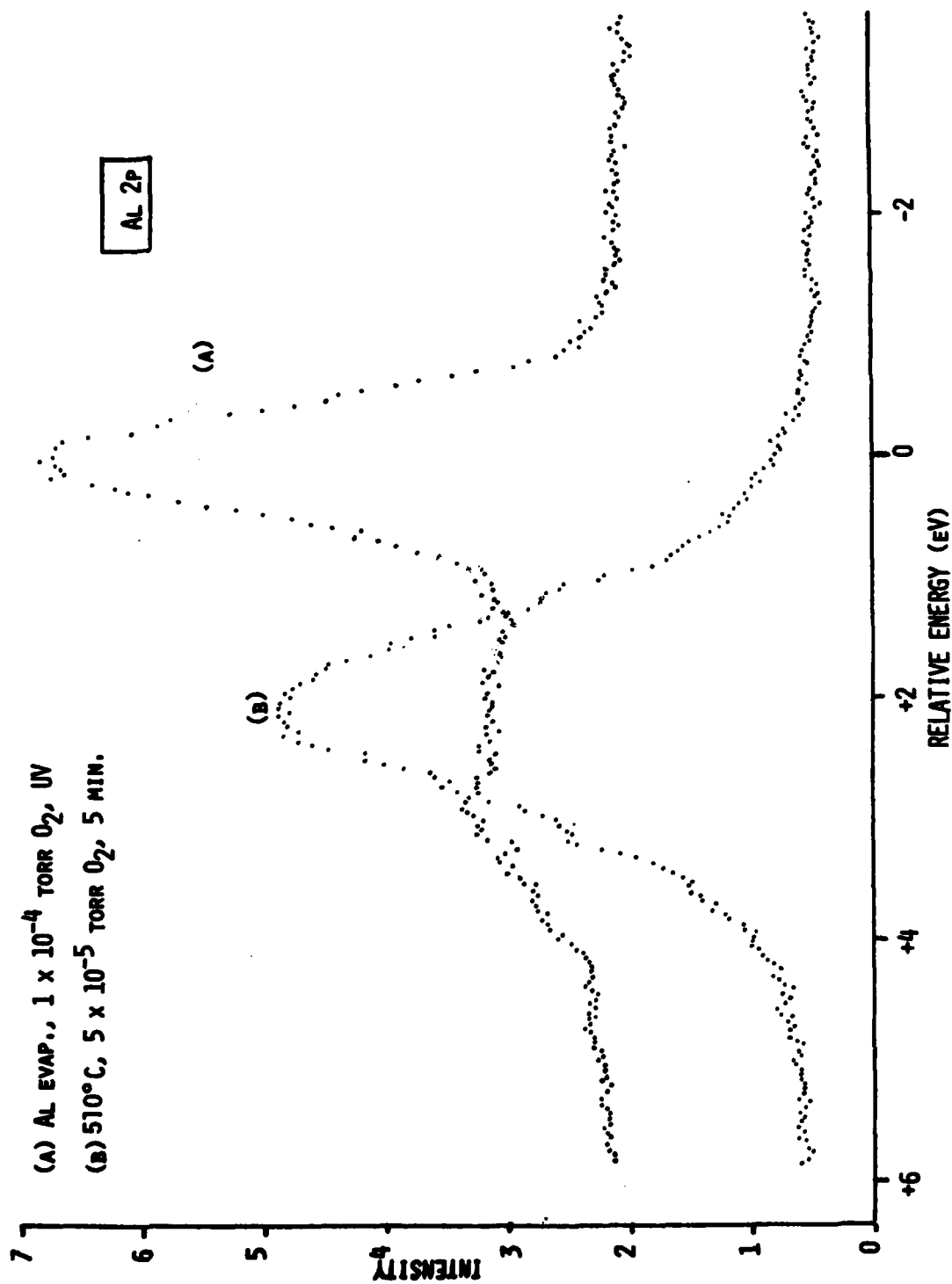


Fig. 5 XPS spectra in region of Al 2p line for (A) evaporation of Al in O_2 with UV light present, and (B) oxidation of Al film in (A) at $510^\circ C$.

(c) 2ND AL EVAP., 1×10^{-4} TORR O_2 , $520^\circ C$
 (d) $520^\circ C$, 5 MIN., 5×10^{-5} TORR O_2

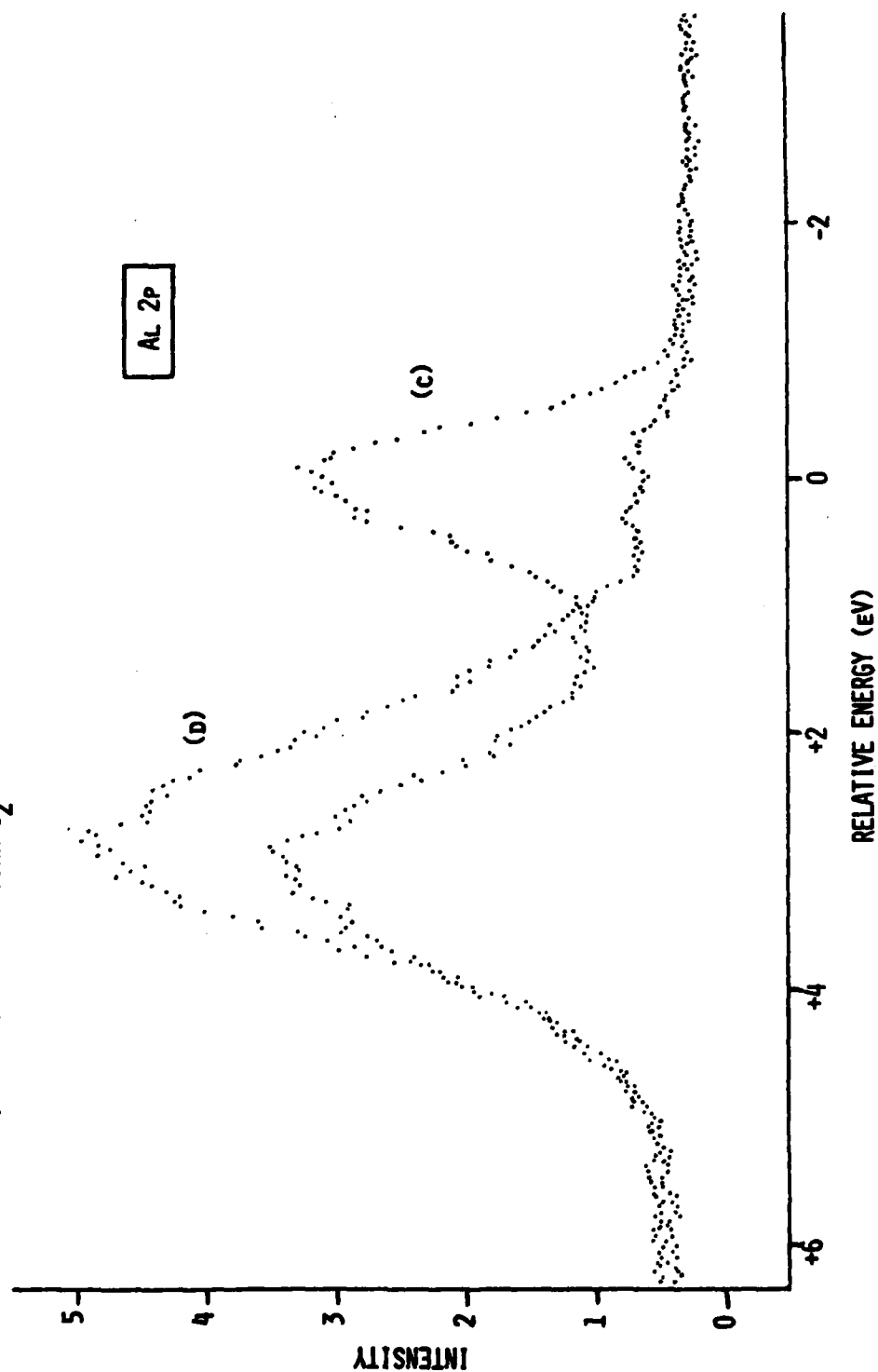


Fig. 6 XPS spectra in region of Al 2p line for (C) additional Al evaporated in O_2 onto the surface characterized as spectrum (B) in Fig. 5 while this surface was at $520^\circ C$ and (D) oxidation of sample in (C) at $520^\circ C$.

(D) 520°C 5 MIN., 5×10^{-5} TORR O_2
 (E) O_2 PLASMA, $\sim 5 \times 10^{-2}$ TORR

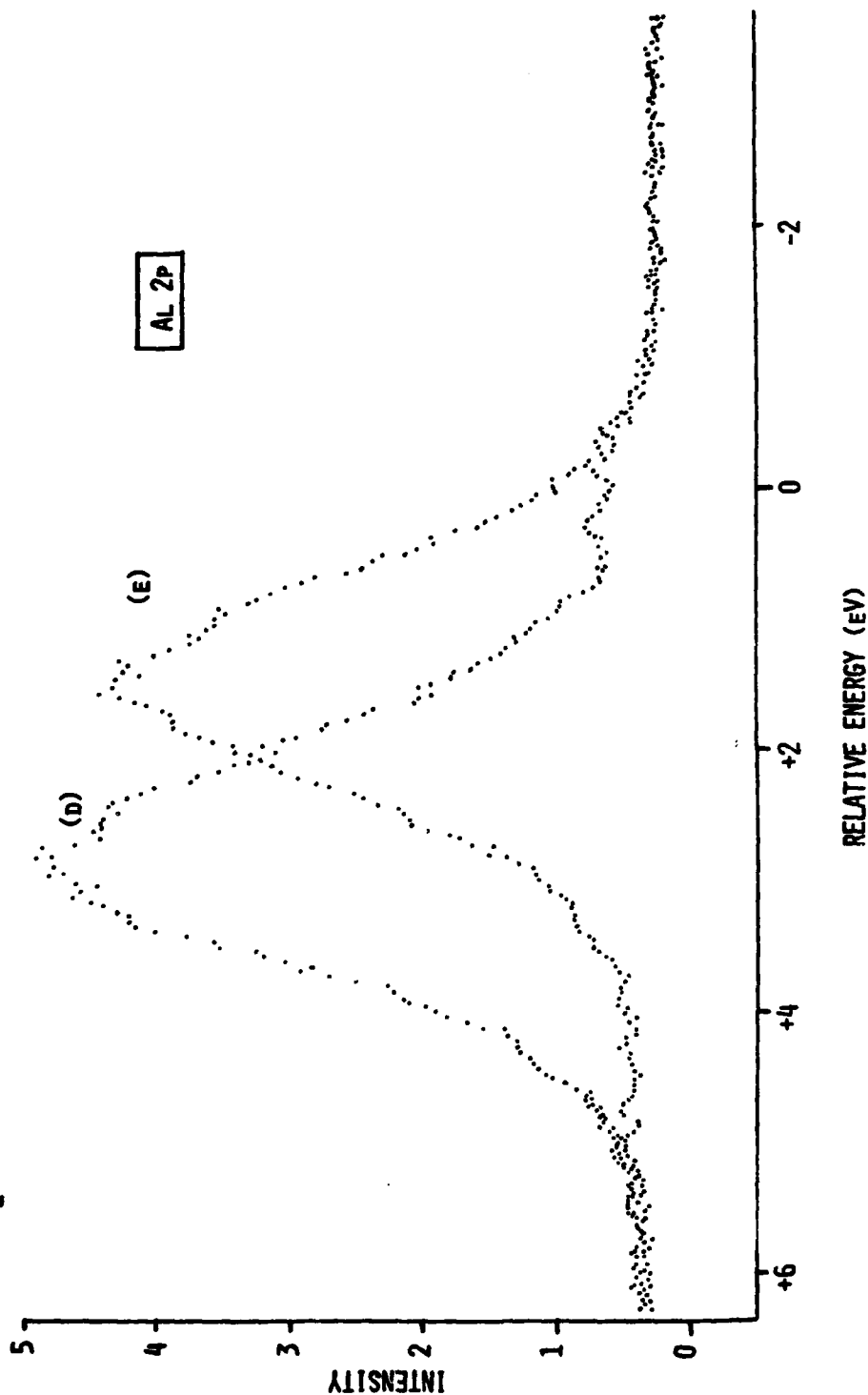


Fig. 7 XPS spectra in region of Al 2p line. Spectrum labeled (D) is repeated from Fig. 6 for reference. Spectrum (E) was obtained after deposition of Al onto the sample at room temperature while in the presence of an O_2 plasma discharge.

third preparation was Al deposition through a plasma discharge in O_2 onto a room temperature substrate. This sample was totally an aluminum oxide, however, the chemical shift was ~ 1.4 eV. The intermediate oxide (with chemical shift of ~ 1.4 eV) is typical of the initial stages of Al metal oxidation at low O_2 exposures^{9,10} and low temperatures.⁸ This is the first observation in which a relatively thick film of the intermediate oxide was prepared at room temperature. These investigations have shown that the oxidation of Al is more complex than might first be expected. It is premature to speculate on the chemical nature of the intermediate Al oxides.

In a previous report,² an investigation of the interaction of Al° with native oxide on GaAs (100) was described. This initial work was extended to include several other metals as part of an independent study. A manuscript based on this work, which has been accepted for publication in Applied Physics Letters, is reproduced in the Appendix. This work will also be discussed in the Physics of Compound Semiconductor Interfaces Conference, January 27-29, 1981.

SECTION III

SAMPLE ANALYSIS

In the first part of this section, C-V and I-V measurements on samples prepared as discussed in Sections II-1 and II-2 are described. To facilitate these measurements, metal dots of 10 and/or 20 mil diameters, were evaporated onto the sample surfaces through a contact mask. The metal dots were ~ 200 Å Cr followed by ~ 2000 Å of Au. The last part of this section describes depth profiles for an oxidized portion of the MBE prepared sample No. 411.

1. C-V and I-V Measurements

a. MBE Samples

One promising approach to making a MIS structure on GaAs with a low interface state density has been to grow a lattice matched $\text{Al}_x\text{Ga}_{1-x}\text{As}$ layer as an insulator.^{1,11} Since such structures typically show large leakage currents, an oxide is grown thermally to seal the structure against such leakage.

As noted in Section II-1 and the last interim report,² we have grown a number of these samples in an attempt to reproduce the results of W.T. Tsang et al¹. C-V curves published by Tsang et al¹ apparently show inversion and accumulation with a low interface state density. However, as discussed in Section IV of this report, these results may be controversial since they give a

smaller change in the surface potential for inversion than expected theoretically.

The results of C-V and I-V measurements on the MBE samples is reported in this section. In the previous interim report² initial studies on sample No. 411 were presented. In this report several new samples labeled No. 490, No. 491, and No. 493 have been investigated. Samples No. 490 and No. 493 are p-type whereas sample No. 491 is n-type.

The results for sample No. 491 are shown in Fig. 8. The C-V plot is reminiscent² of data taken for sample No. 411. There is a large hysteresis which depends on the direction of the scanning voltage. This hysteresis is consistent with charge storage at the interface and has been discussed in the previous report.² The effect of a longer oxidation anneal is shown in the figure. There is only a small change between a 200 min and a 1040 min oxidation which indicates a slightly thicker insulator for the longer oxidation. These results indicate a complete oxidation of the AlAs and suggest that a significant portion of the $\text{Al}_{1-x}\text{Ga}_x\text{As}$ is also oxidized under these conditions.

The I-V measurements for sample No. 491 with a 200 min oxidation indicate a leakage current of 10^{-9} amps at 6 volts forward bias for a 20 mil dia. dot. The thickness of the insulating layer is not known but can be estimated to be in excess of 2000 Å.

The C-V characteristics for sample 490 are indicated in Fig. 9. Although at first glance the sample appears to be going into inversion, further analysis has shown that a more likely explanation is that the sample

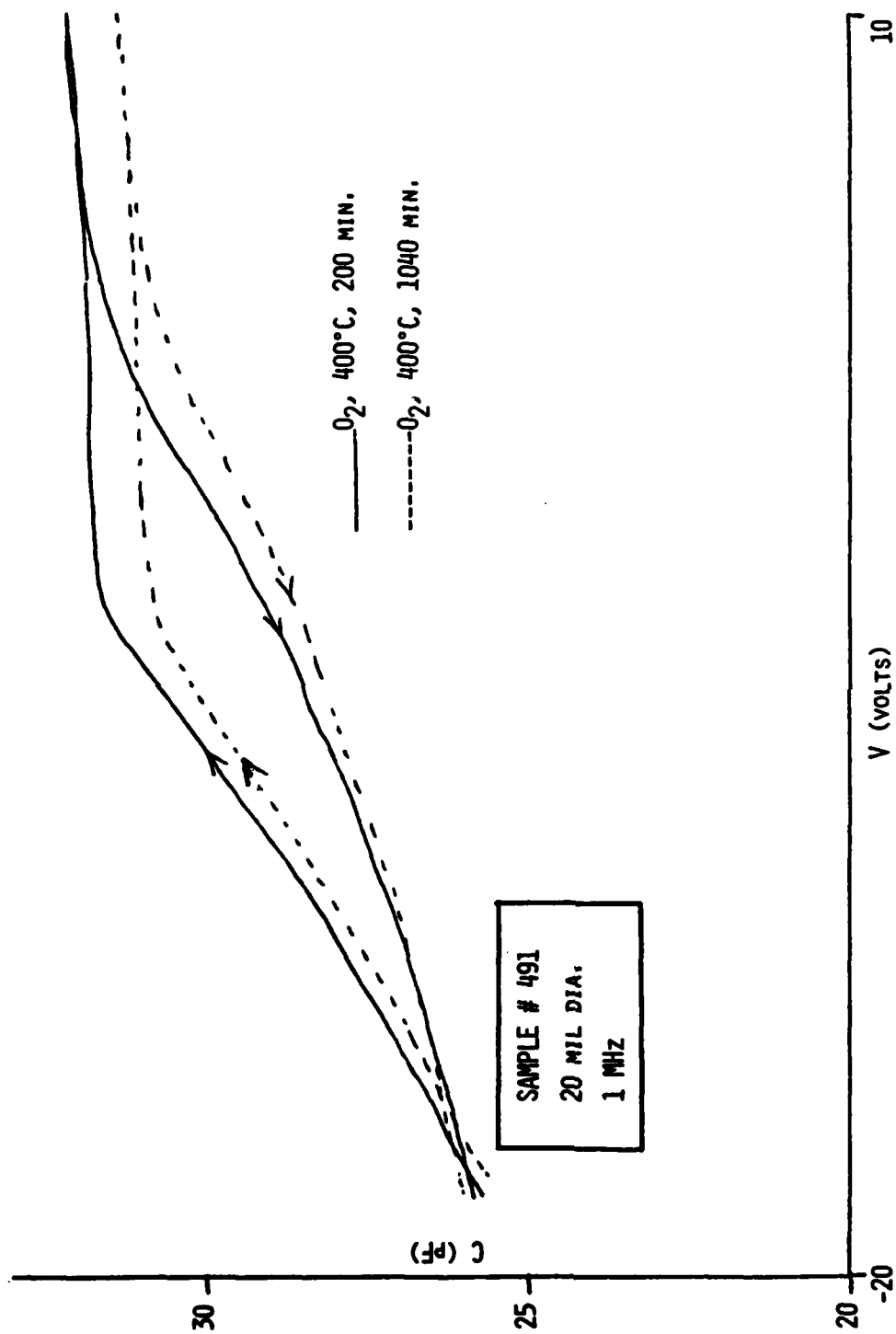


Fig. 8 C-Y measurements for Sample No. 491.

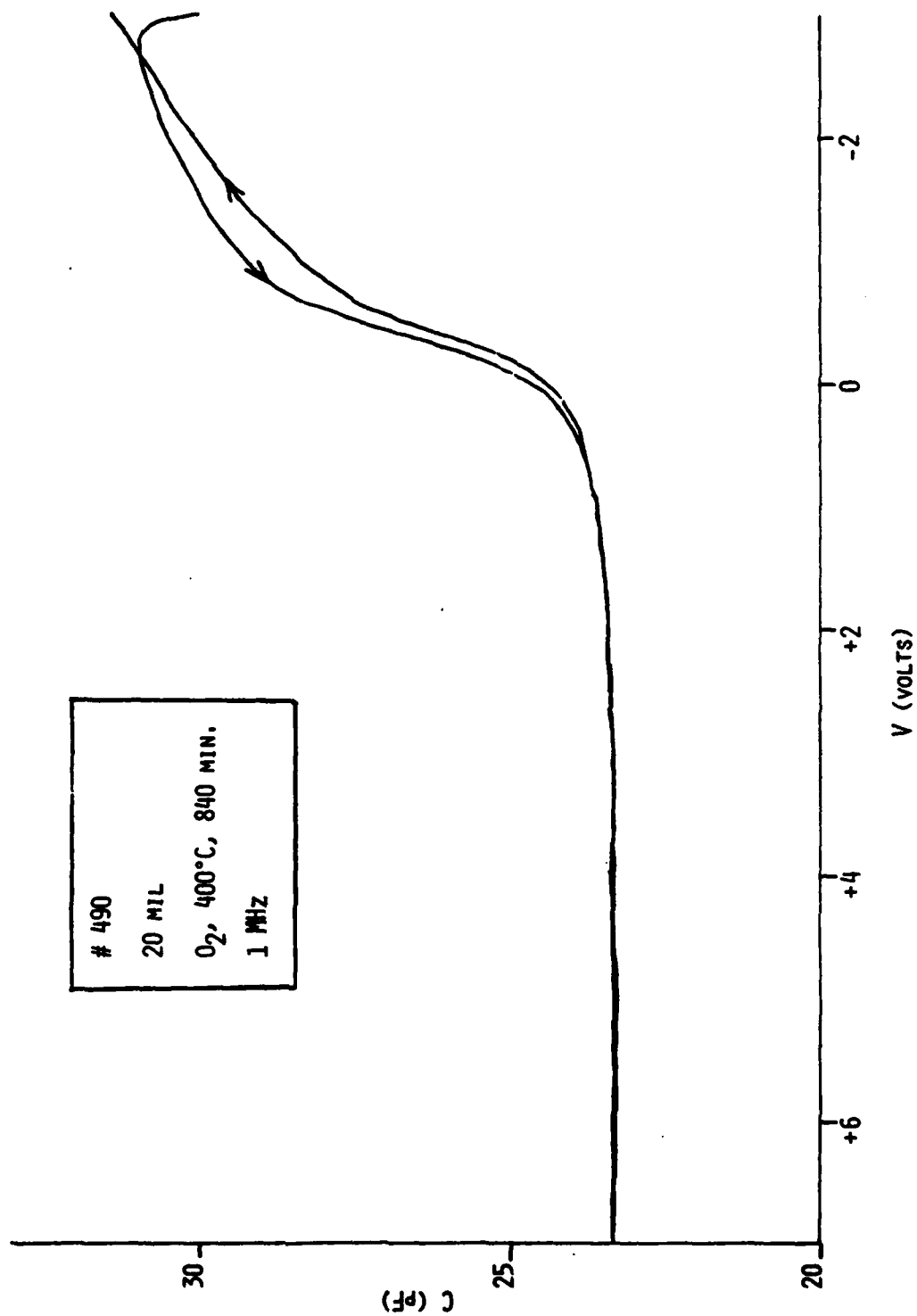


Fig. 9 C-V measurements for Sample No. 490.

has depleted through to the substrate. Such an interpretation was shown to be correct by analyzing the C-V characteristics for a device with the thermal oxide removed and a contact to the $\text{Al}_{1-x}\text{Ga}_x\text{As}$ epilayer. The device was very leaky but yielded a capacitance consistent with the width of the GaAs layer.

Sample No. 493 was similar to No. 490 but with a thicker, more heavily doped GaAs layer. C-V measurements are shown in Fig. 10. There is a small flat-band voltage shift of -0.6 volts for these samples which indicates a positive interface charge. The samples show a small amount of hysteresis but do not give any indication of inversion. The I-V curves indicate breakdown at very low forward voltages of about -2 to -4 volts. Typically for a forward voltage of -2 volts, currents of 3×10^{-8} amps are observed for a 20 mil diameter device. The thickness of the insulator is not known with great certainty.

In the previous interim report,² preparation and initial characterization of the MBE grown sample No. 411 was described (this sample is an attempt to reproduce the structure reported in Ref. 1). A portion of this sample was oxidized sequentially for increasing lengths of time in an attempt to move the oxide interface through the $\text{Al}_{1-x}\text{Ga}_x\text{As}$ layer. After each sequential oxidation a row of 10 mil dia dots was evaporated onto the sample and C-V measurements were carried out at 1 MHz. The total accumulated oxidation times were 10, 60, 330, 1575, and 10,455 min respectively. C-V measurements on the initial sample (this sample has been superficially oxidized for ≈ 0.5 min and stored in a vacuum box since preparation) showed considerable nonuniformity in behavior for different capacitors. A selected example is shown in Fig. 11

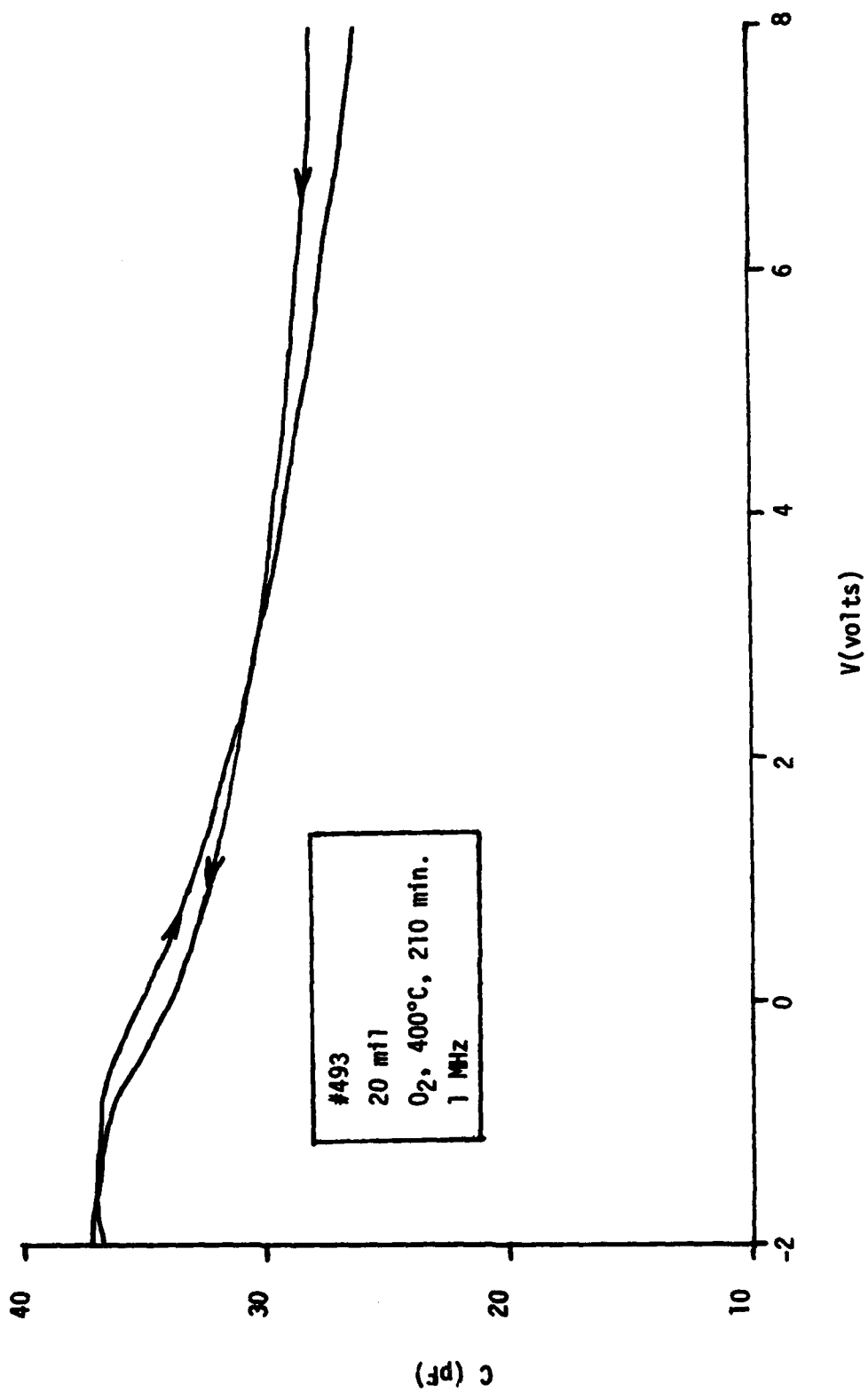


Fig. 10 C-V measurements for Sample No. 493.

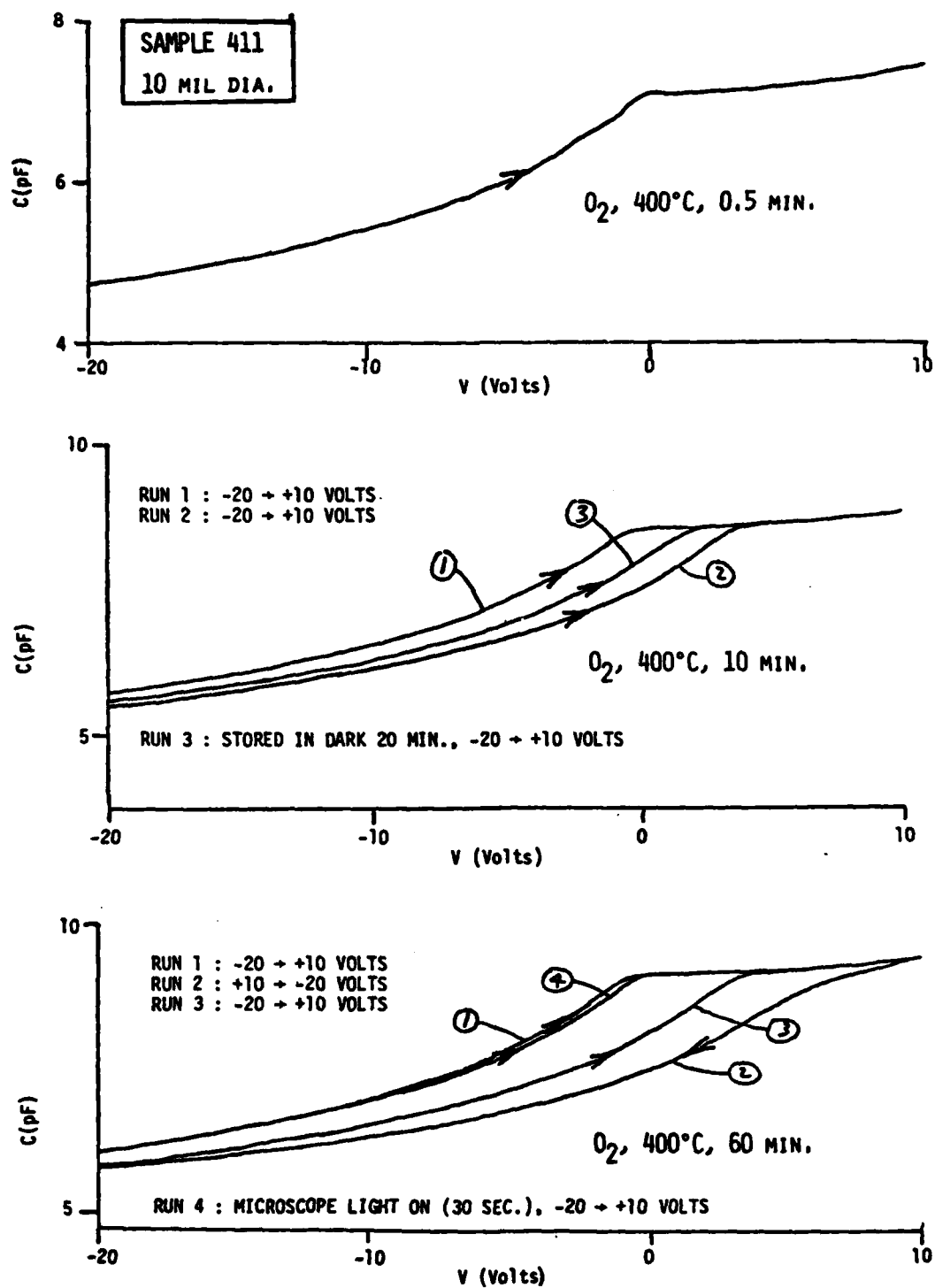


Fig. 11 C-V measurements at 1 MHz for sample No. 411 after three sequential oxidations, (top) 0.5 min oxidation, (middle) 10 min oxidation, and (bottom) 60 min oxidation.

(top). For the other five series of experiments, the uniformity of characteristics was markedly better. In Fig. 11 (middle), a C-V measurement is shown following the 10 min oxidation. The "oxide" capacitance has increased substantially and there is a large hysteresis and shift of the flat-band voltage due to interface charge storage (the interface charge decreases noticeably after storage in the dark for many minutes). Figure 11 (bottom) is a C-V measurement after 60 min of oxidation. Little change in characteristics was observed as compared to the 10 min oxidation. It was observed that the charge storage effect could be "erased" by exposure to microscope light. Figure 12 (top) is a C-V measurement taken after 330 min of oxidation. Little change in the C-V characteristics was observed as compared to the previous 2 sets of measurements. It was observed that the flat-band voltage was nearly a linear function of forward-bias voltage applied to the sample. Figure 12 (bottom) is a C-V measurement obtained after 1575 min of oxidation. The C-V characteristics are similar to the results for the previous 3 sets of measurements, although an increase in oxide capacitance is observed which may be significant. Figure 13 shows C-V measurements obtained after 10,455 min of oxidation. The devices after this amount of oxidation were considerably more leaky than the previous devices and forward breakdown occurred at ≈ 8 volts. A depth profile of this sample taken after the 10,455 min oxidation is reported in Section III-2.

In summary, sample No. 493 shows the most satisfactory C-V curves, showing minimal hysteresis compared to the other structures. A persistent problem with these devices is that the thermal oxide is very leaky,

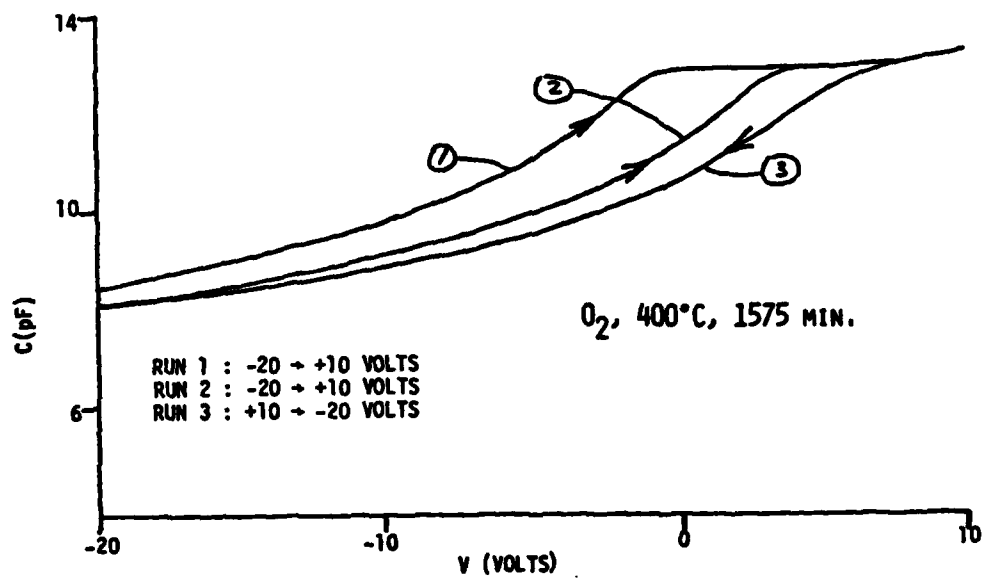
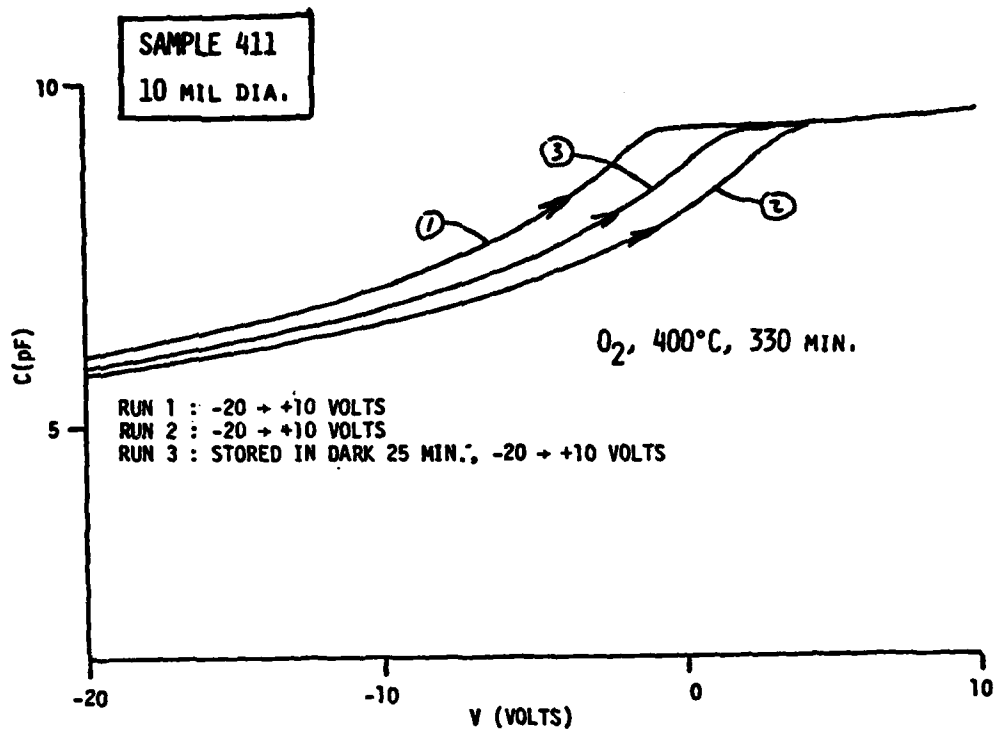


Fig. 12 C-V measurements at 1 MHz for same sample as in Fig. 11, (top) 330 min oxidation, (bottom) 1575 min oxidation.

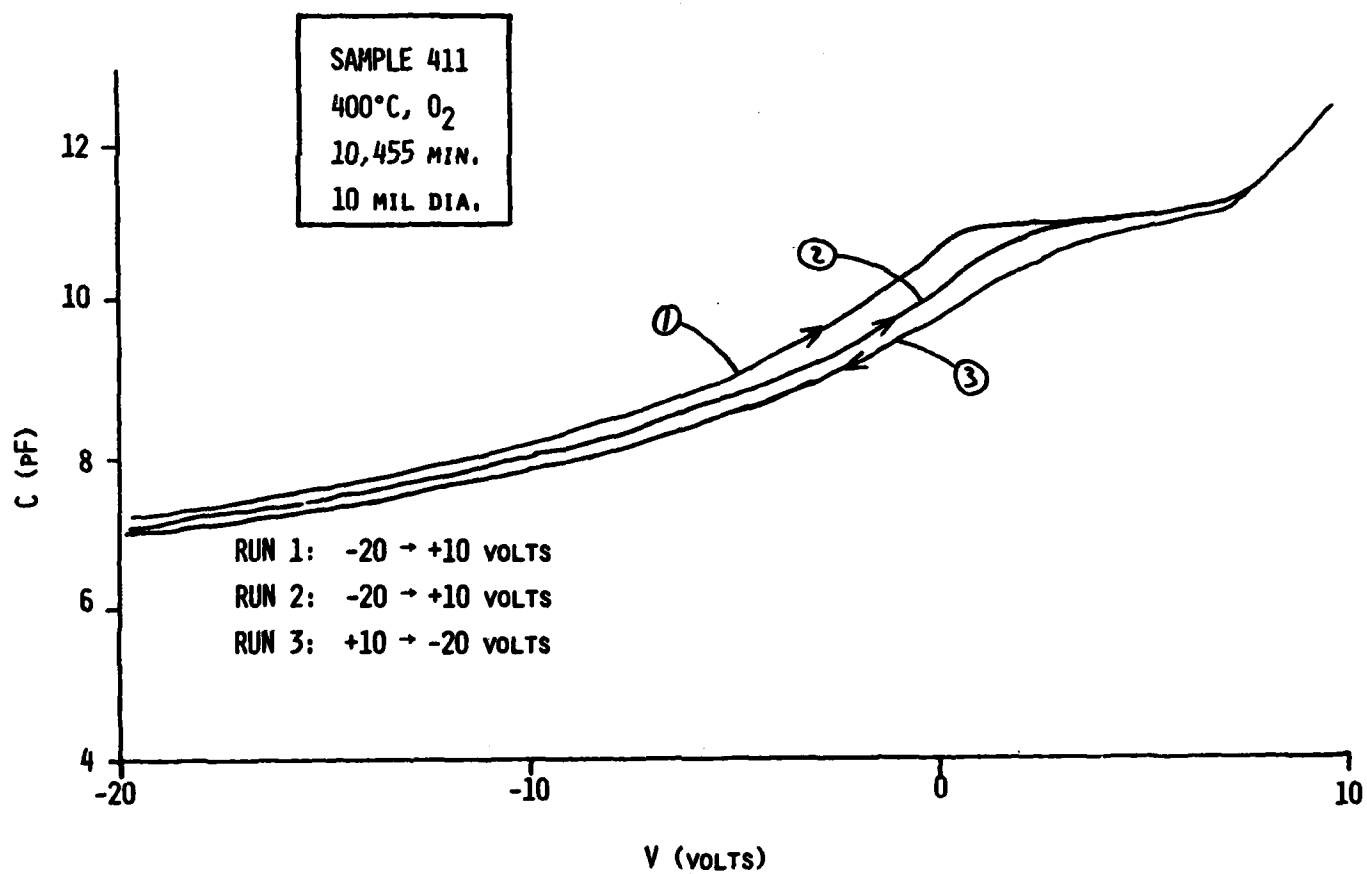


Fig. 13 C-V measurements at 1 MHz for same sample as in Figs. 11 and 12 after 10,455 min oxidation.

effectively preventing inversion in any of the devices at present. One approach which is being investigated is the use of various other insulators as a substitute for the thermal oxide.

b. Deposited Insulator Samples

As discussed in Section II-2 several samples were prepared and studied after SiO_x deposition in the XPS apparatus. Results of C-V and I-V measurements on these samples are presented here. Both p-type and n-type samples were prepared.

In the first of these samples, X1, a few monolayers of Ga_2O_3 were formed by heating the GaAs surface to $\sim 460^\circ\text{C}$ during exposure to 6×10^4 L of oxygen. This was followed by vacuum evaporation of ~ 1000 Å of SiO_x . Metal dots were subsequently evaporated onto the samples and 1 MHz C-V measurements and I-V measurements were performed.

Typical results are shown in Fig. 14 for C-V measurements on these samples. For the p-type sample a deep depletion curve is observed for a large positive bias. Although the estimated change in the surface potential is large enough for inversion to occur, leakage through the oxide apparently prevents accumulation of electrons in the inversion layer.¹² At reverse bias the device appears to go into accumulation. The n-type sample shows a C-V curve which is not interpretable by standard methods. Although the curve shows some indication of deep depletion, no accumulation or inversion behavior is identifiable.

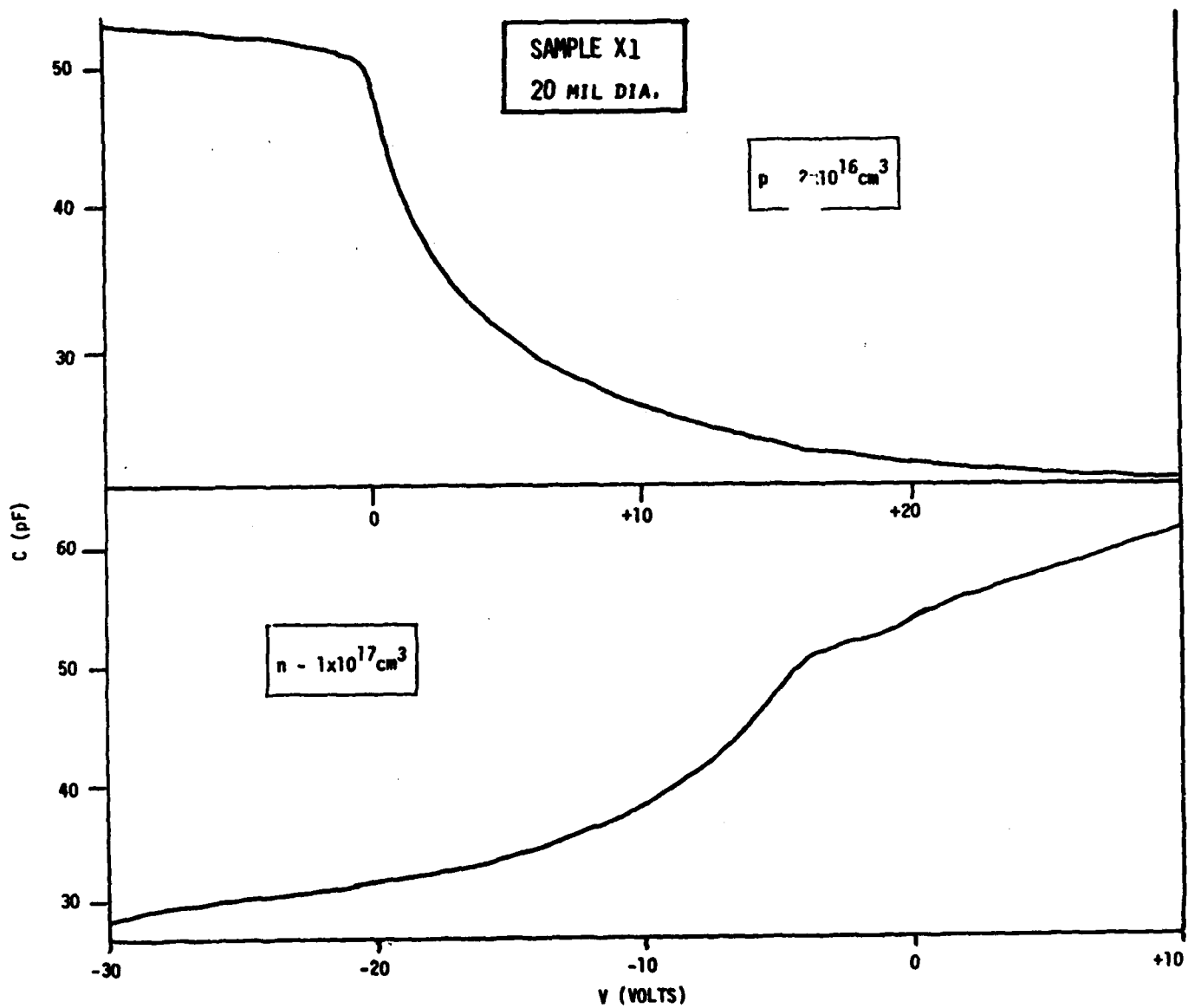


Fig. 14 C-V measurements at 1 MHz for sample X1.

Characteristic I-V curves for the p-type samples are shown in Fig. 15. Under forward bias the electric field is across the insulator and a relatively high current density is observed at relatively low fields (5×10^{-5} amps/cm² for 2×10^5 V/cm). This behavior is consistent with the absence of inversion in the C-V measurements.

Samples X2 through X5 were made by depositing SiO_x photochemically on the GaAs as described in Section II-2. As shown in Fig. 16 this oxide showed superior dielectric properties compared to the evaporated SiO_x. In this figure the I-V characteristics are shown for two devices produced with similar oxide thicknesses by vacuum evaporated and photochemically produced SiO_x. The device with the SiO_x photochemically produced oxide has a leakage current which is two orders of magnitude less than the device with the evaporated SiO_x. Although there is considerable scatter in leakage currents between devices, the better devices produced by the two techniques consistently exhibited this trend.

It was hoped that the superior dielectric properties of the photochemically produced SiO_x would yield devices which would show inversion without hysteresis in the C-V characteristics. This did not turn out to be the case. Some typical C-V curves are shown in Figs. 17-20 for these samples. Most of the C-V curves are not directly interpretable. Those which are interpretable show deep-depletion and considerable hysteresis. One possible explanation for this behavior is that the leakage current through the oxide eliminates charging of the semiconductor interface and the consequent hysteresis associated with slow interface states.

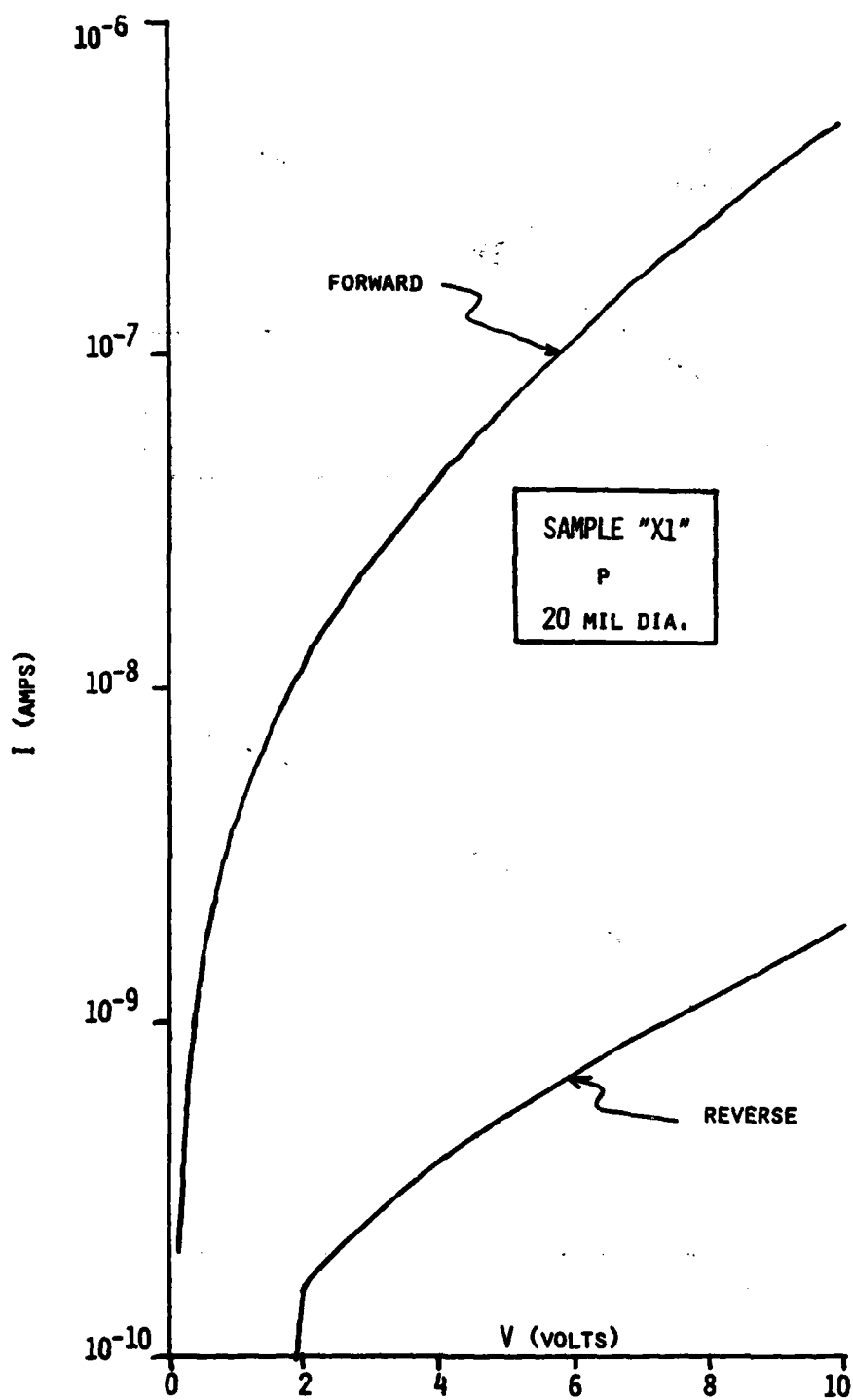


Fig. 15 I-V measurements for sample X1 (p-type).

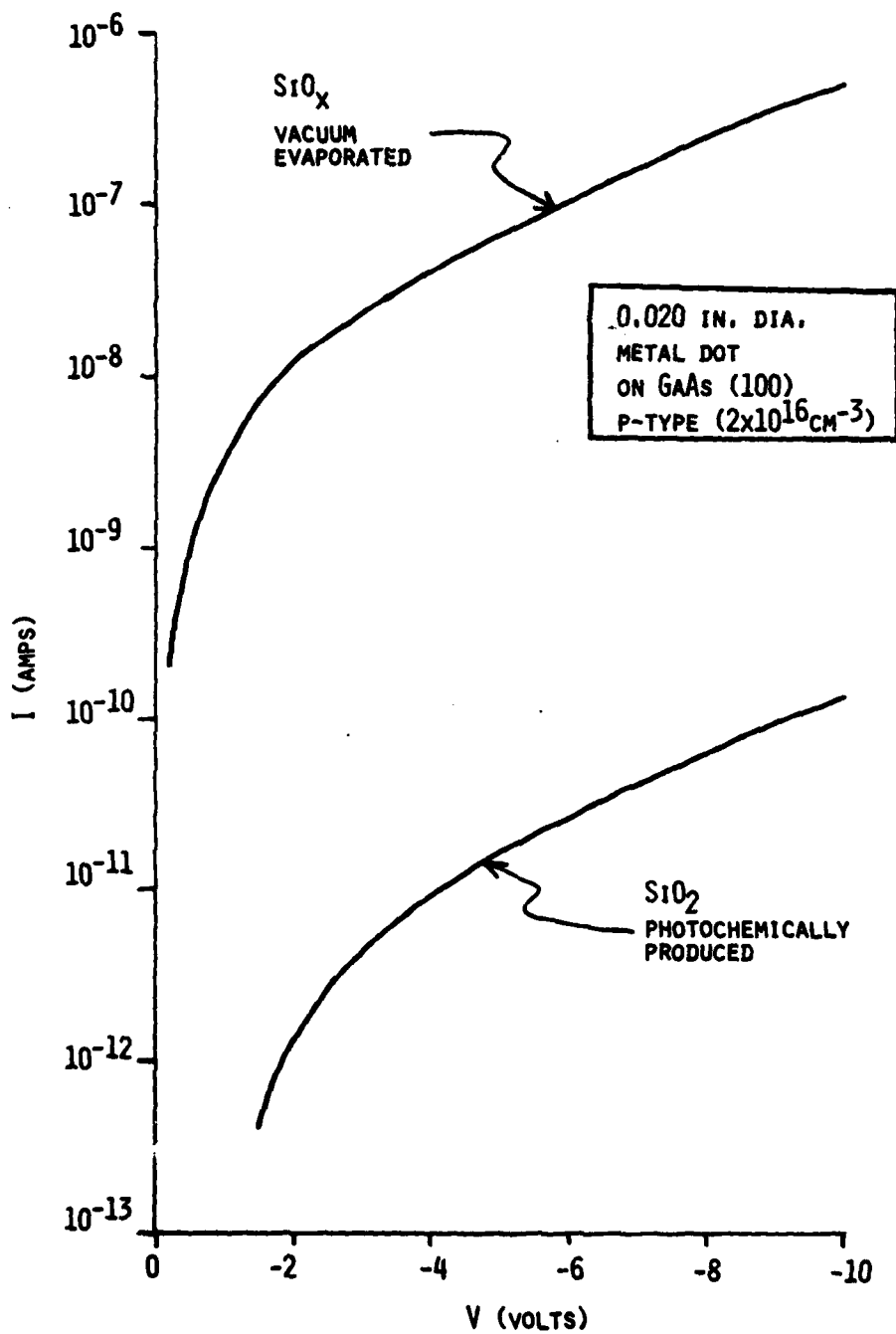


Fig. 16 Comparison of leakage currents for vacuum evaporated SiO_x and photochemically produced SiO_2 insulators.

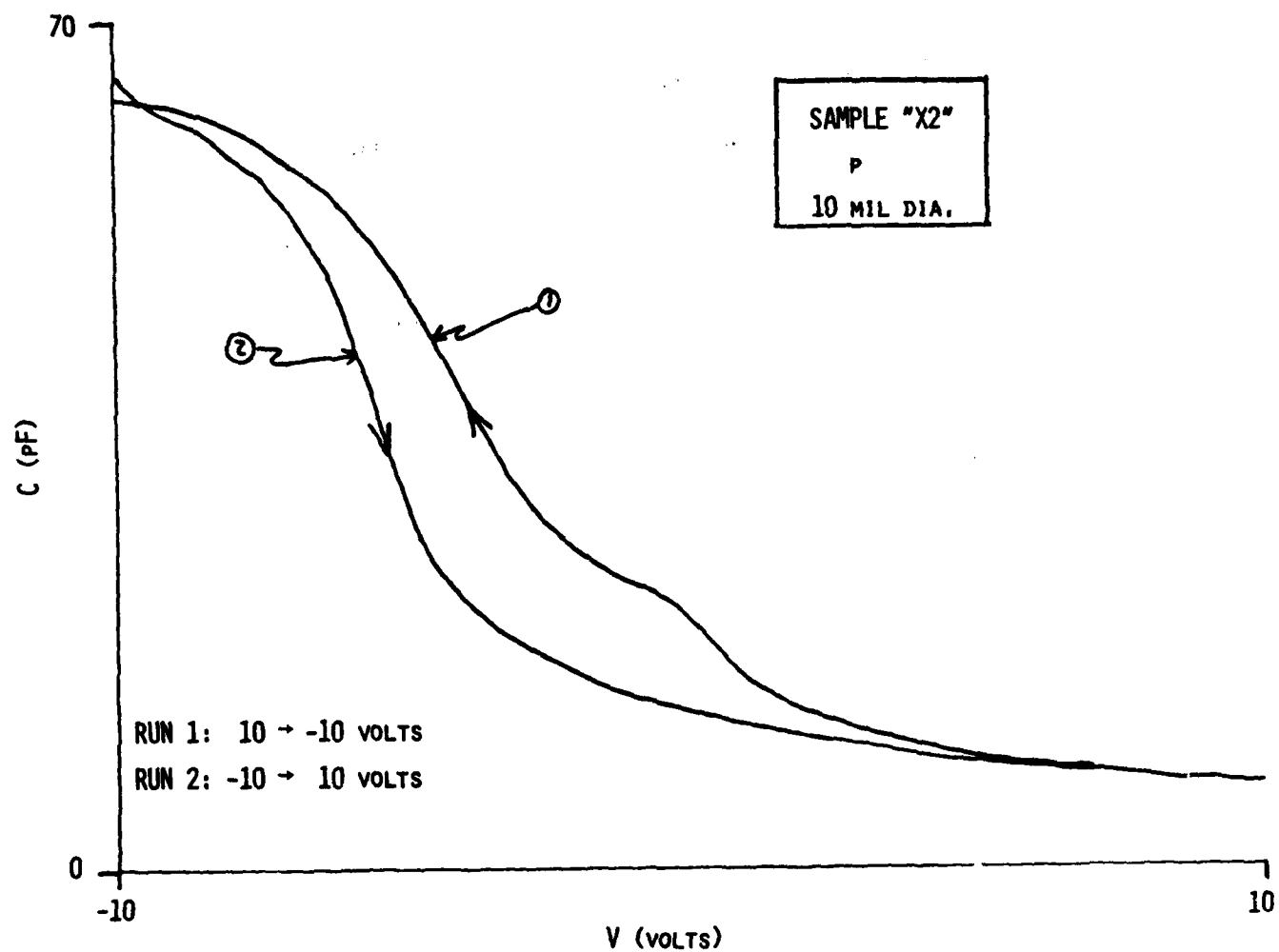


Fig. 17 C-V measurements at 1 MHz for sample X2 (p-type).

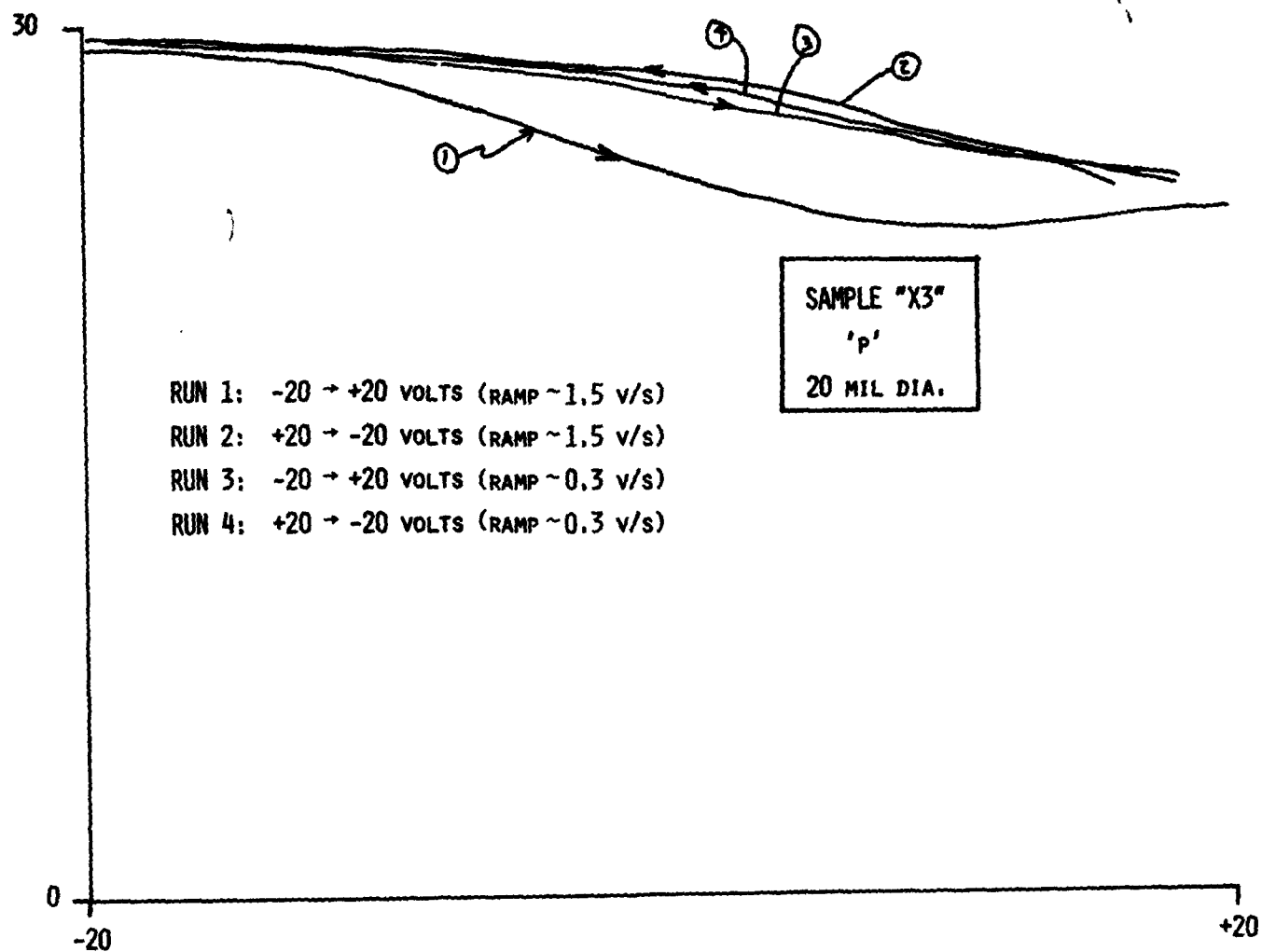


Fig. 18 C-V measurements at 1 MHz for sample X3 (p-type).

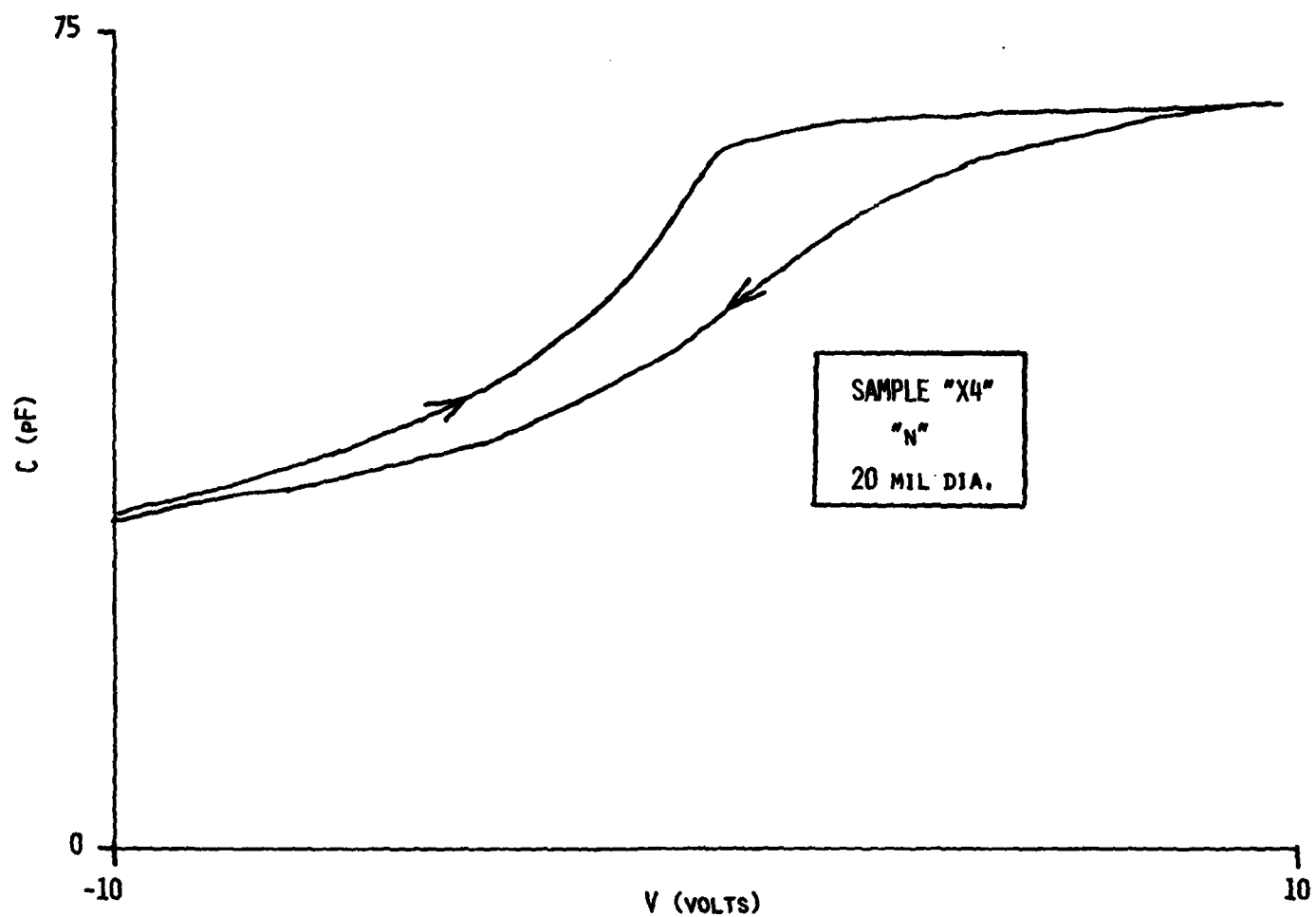


Fig. 19 C-V measurements at 1 MHz for sample X4 (n-type).

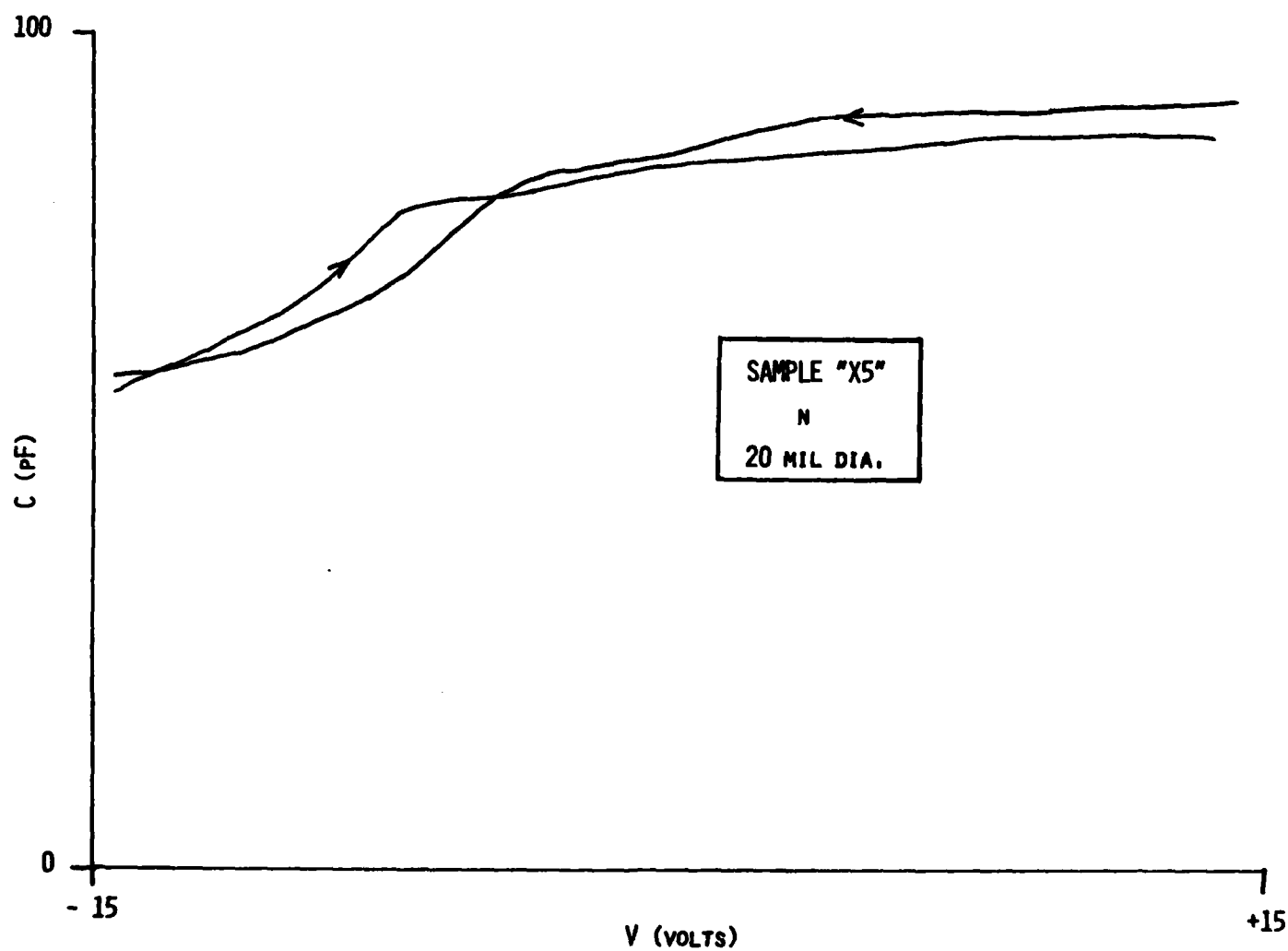


Fig. 20 C-V measurements at 1 MHz for sample X5 (n-type).

One of the samples, X3, which showed good leakage characteristics was sent for evaluation to Dr. B. Bayraktaroglu at the Air Force Wright Aeronautical Laboratories (AFSC) where frequency dependent C-V and G-V measurements were made.¹³ Hysteresis in the C-V and G-V curves was observed. The C-V curves were difficult to study due to the small change in capacitance with applied voltage. The G-V curves produced distinct peaks at all test frequencies. Such peaks indicate the presence of states at the interface. Typical examples of some of these data are shown in Figs. 21 and 22.

In conclusion, none of the SiO_x insulating layers currently investigated was capable of satisfactorily passivating the GaAs surface suitably for device applications. Inversion was not observed for any device while only devices with unacceptably large leakage showed interpretable C-V curves without hysteresis.

2. Depth Profile of Sample No. 411

At the conclusion of the series of sequential oxidations carried out on Sample No. 411 (see Sections II-1 and III-1-a) a scanning Auger microprobe (SAM) depth profile was obtained by a series of sputter-Auger analysis steps. The SAM instrumentation has been previously described.² The result of this Ar^+ sputtering depth profile is presented in Fig. 23.

The sputter time axis of Fig. 23 is related to depth within the sample and the sputter rate is $\sim 20 \text{ \AA/min}$. The graded $\text{Al}_{1-x}\text{Ga}_x\text{As}$ layer is

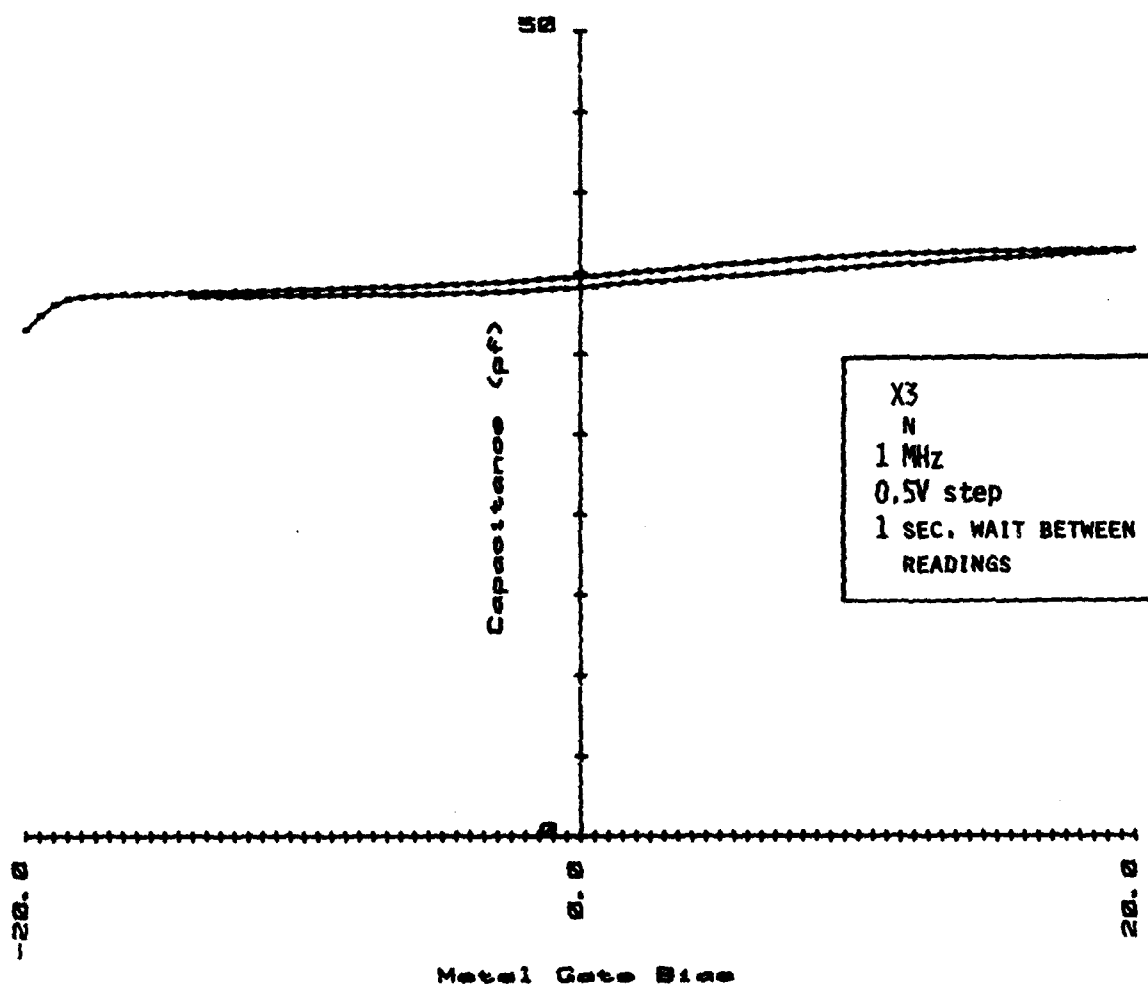


Fig. 21 C-V measurements at 1 MHz for sample X3 (n-type). Data obtained by B. Bayraktaroglu (WPAFB).

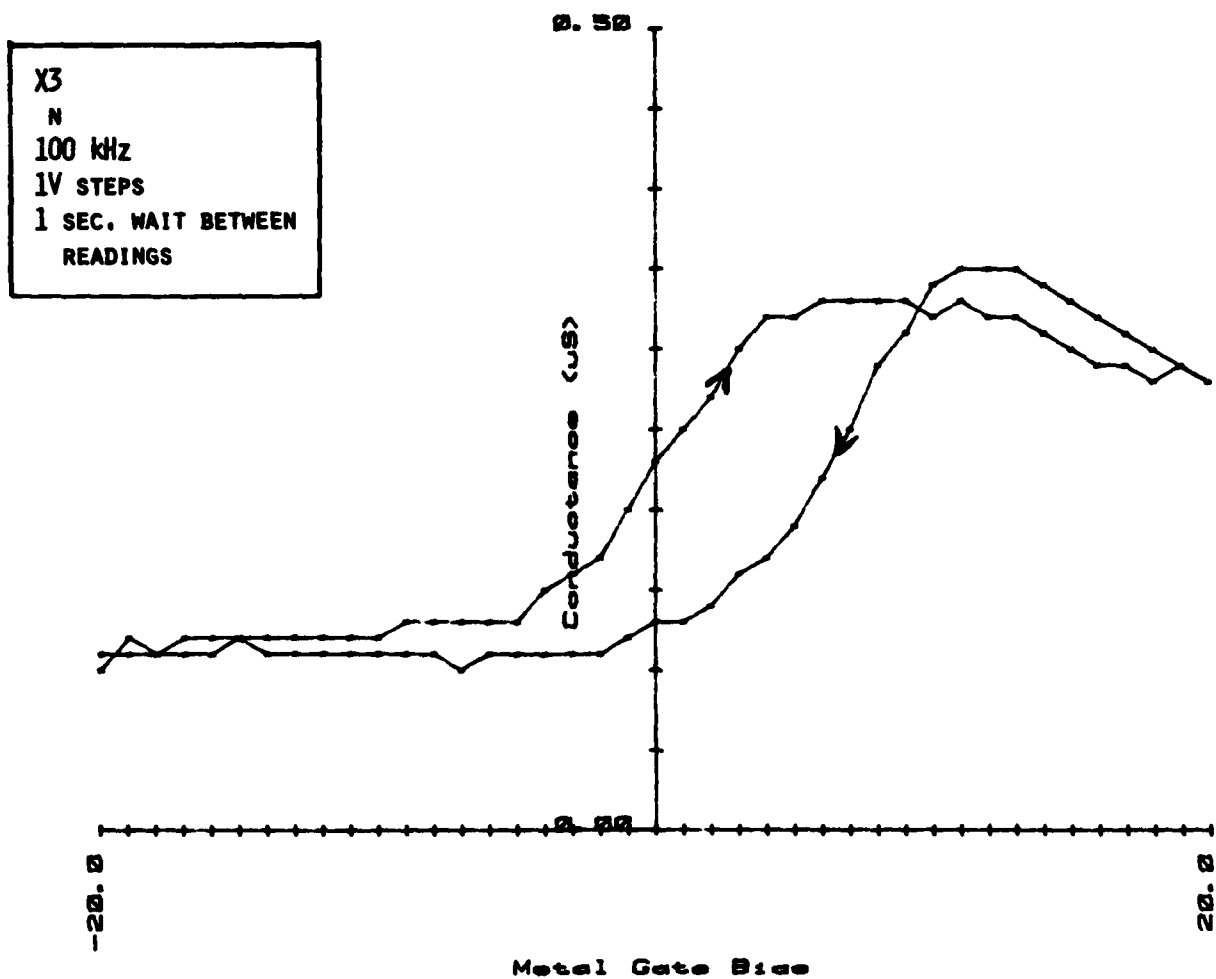


Fig. 22 G-V measurements at 100 kHz for sample X3 (n-type). Data obtained by B. Bayraktaroglu (WPAFB).

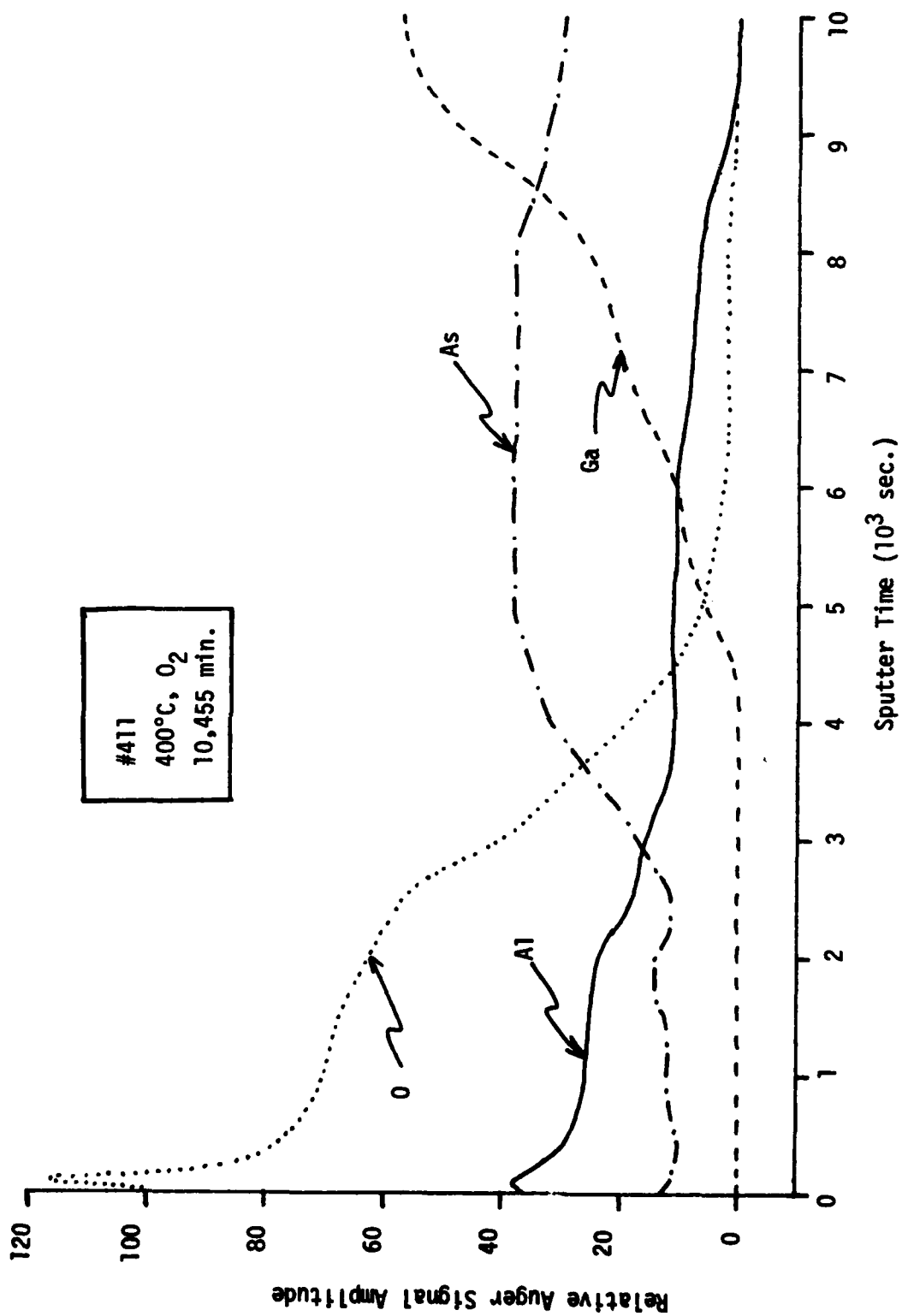


Fig. 23 Depth profile obtained with SAM for sample #411 after oxidation in O₂ at 400°C for 10,455 min.

reached after sputtering $\sim 4 \times 10^3$ s while the GaAs layer is reached after $\sim 9 \times 10^3$ s of sputtering. The important result is that the oxygen signal extends all the way to the GaAs layer and seems to decrease at approximately the same rate as the Al signal. Therefore, after 10,455 min of oxidation, this sample appeared to be oxidized completely through the graded $\text{Al}_{1-x}\text{Ga}_x\text{As}$ layer.

An XPS depth profile was also obtained on this same sample. Difficulties experienced in aligning the sputter crater and the x-ray beam made this profile a bit more difficult to interpret although the basic conclusions are the same as those drawn from the SAM profile (Fig. 23). The XPS data obtained within the graded $\text{Al}_{1-x}\text{Ga}_x\text{As}$ layer showed that the Al was oxidized while the Ga was not oxidized. Although this result could be an artifact of the sputtering process our previous experience suggests that this explanation is unlikely.

SECTION IV

DISCUSSIONS OF PREVIOUS MBE RESULTS

In view of our (and others)¹⁴ difficulty in reproducing the C-V results for the MBE grown structures reported by Tsang et al,¹ we have re-examined the published data and find some apparent internal inconsistency. In Fig. 24 the published C-V data of Tsang et al is reproduced. Additional stated parameters are: $2 \times 10^{-3} \text{ cm}^2$ Au dot, $C_i = 3.7 \times 10^{-8} \text{ F/cm}^2$, $N_D = 8 \times 10^{16} \text{ cm}^{-3}$, where C_i is the measured insulator capacitance and N_D is the active GaAs layer doping. Since the data look very close to an ideal C-V curve, we will use only the elementary analysis applicable to an ideal MOS structure. For example, at inversion, the data show $C/C_i = 0.7$, where C is the total MOS capacitance. This immediately implies that at inversion the capacitance of the semiconductor is:

$$C_S^{\text{inv}} = \frac{\left(\frac{C}{C_i}\right)}{1 - \left(\frac{C}{C_i}\right)} C_i = \frac{0.7}{0.3} C_i = 8.6 \times 10^{-8} \text{ F/cm}^2 .$$

For a semiconductor, the AC capacitance at inversion is:

$$C_S^{\text{inv}} = \epsilon_S / W_m$$

where W_m is the depletion width and $\epsilon_S = 1.11 \times 10^{-12} \text{ F/cm}^2$, the dielectric constant for GaAs. Thus, $W_m = 1.11 \times 10^{-2} / 8.6 \times 10^{-8} = 1.29 \times 10^{-5} \text{ cm} = 1290 \text{ \AA}$ is the measured value for W_m .

This value for W_m must be consistent with:

$$W_m = (2\epsilon_S V_S^{\text{inv}} / qN_D)^{1/2}$$

which is the depletion width at inversion as a function of doping. For GaAs, $V_S^{\text{inv}} \sim 1.4 \text{ V}$, thus,

$$N_D = 2\epsilon_S V_S^{\text{inv}} / qW_m^2 = 1.13 \times 10^{17} \text{ cm}^{-3}$$

is the actual measured value for N_D . This is consistent with the stated value of $8 \times 10^{16} \text{ cm}^{-3}$.

The other parameter directly available from Fig. 24 is the gate voltage, V_g , at inversion, which is measured as $\sim 2.1 \text{ V}$. This value of V_g should be compatible with:

$$V_g = (Q_B/C_i) + V_S^{\text{inv}} ,$$

$$Q_{ss} \sim 2 \times 10^{10} \text{ cm}^{-2}$$

$$V_{FB} = 0-0.1 \text{ V}$$

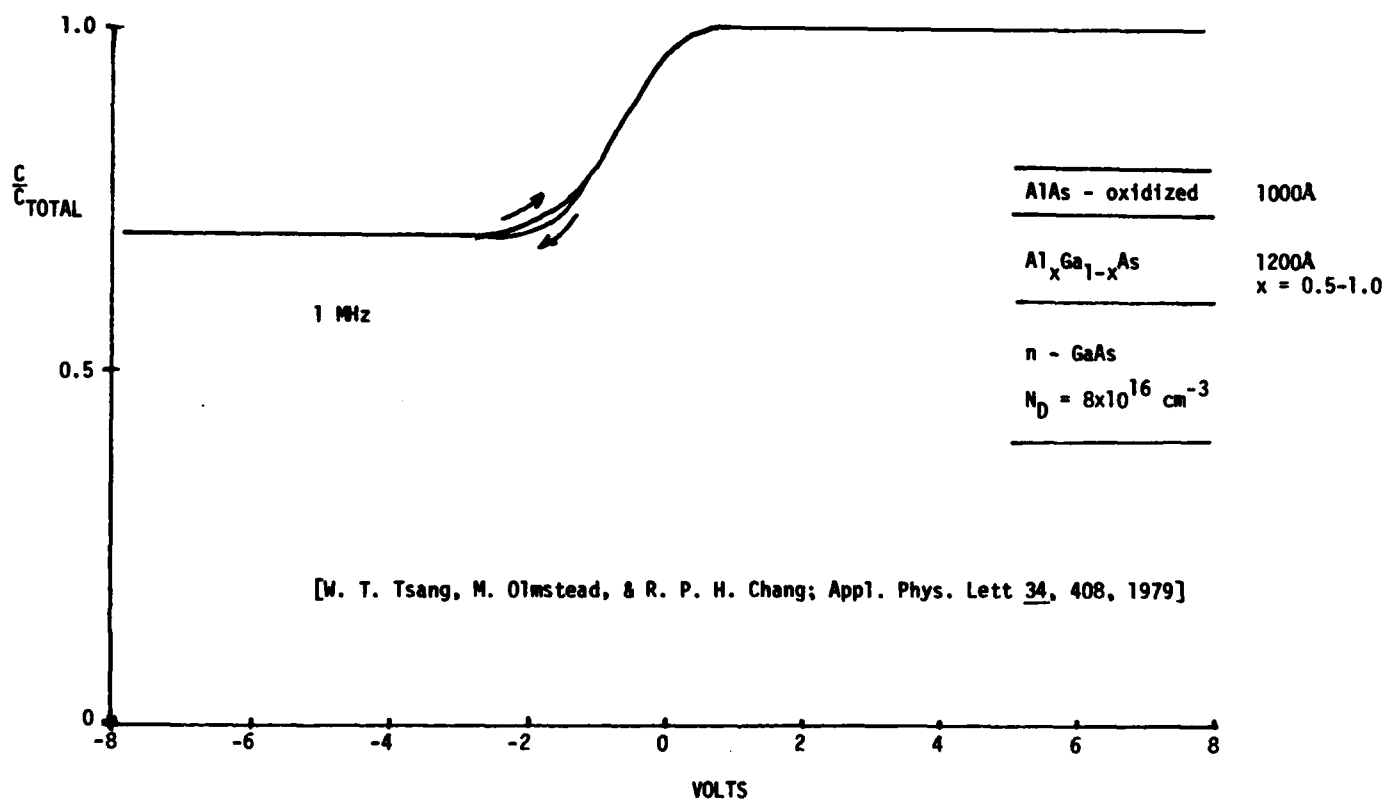


Fig. 24 C-V measurements for thermally oxidized MBE grown sample of AlAs/graded $\text{Al}_x\text{Ga}_{1-x}\text{As}$ /GaAs replotted from Ref. 1.

which states that the voltage across the insulator and semiconductor equals the gate voltage at inversion, $Q_B = (2\epsilon_S q N_D V_S^{inv})^{1/2} = 2.3 \times 10^{-7} \text{ coul/cm}^2$. Thus $(Q_B/C_i) = 6.3 \text{ V}$ (5.4 V for the quoted $8 \times 10^{16} \text{ cm}^{-3}$ doping). In the absence of significant interface charge, which the data show to be the case, this simple analysis indicates that although the capacitance values measured for "flatband" and "inversion" are consistent with the stated oxide thickness and n-type layer doping, the gate bias at inversion should be $\sim 7 \text{ V}$ rather than the $\sim 2 \text{ V}$ shown. Interface charge would increase V_g , thus our calculated V_g is a minimum value. We presently have no explanation for the low gate voltage at inversion shown in the data.

REFERENCES

1. W.T. Tsang, M. Olmstead, and R.P.H. Chang, Appl. Phys. Lett. 34, 408 (1979).
2. R.W. Grant, J.R. Oliver, S.P. Kowalczyk, J.R. Waldrop and D.L. Miller, Technical Report AFWAL-TR-80-1104.
3. R. Dingle, W. Wiegmann, and C.H. Henry, Phys. Rev. Lett. 33, 827 (1974).
4. R.W. Grant, S.P. Kowalczyk, J.R. Waldrop, and W.A. Hill, in The Physics of MOS Insulators, p. 202 (Pergamon Press, New York, 1980) edited by G. Lucovsky, S.T. Pantelides, and F.L. Galeener.
5. T. Adachi and C.R. Helms, J. Electrochem Soc. 127, 1617 (1980).
6. S. Yokoyama, K. Yukitomo, M. Hirose, and Y. Osaka, Thin Solid Films 56, 81 (1979).
7. P. Kofstad, High-Temperature Oxidation of Metals (Wiley, New York, 1966).
8. A.F. Carley and M.W. Roberts, Proc. R. Soc. Lond A363, 403 (1978).

9. S.A. Flodstrom, R.Z. Bachrach, R.S. Bauer, and S.B.M. Hagstrom["], Phys. Rev. Letters 37, 1282 (1976).
10. A. Bianconi, R.Z. Bachrach, S.B.M. Hagstrom["] and S.A. Flodstrom, Phys. Rev. B19, 2837 (1979).
11. H.C. Casey, Jr., A.Y. Cho, and E.H. Nicollian, Appl. Phys. Lett. 32, 678 (1978).
12. For a discussion of C-V measurements and their interpretation, see A.S. Grove, B.E. Deal, E.H. Snow, and C.T. Sah, Solid St. Electronics 8, 145 (1965).
13. G-V measurements are discussed in the literature by E.H. Nicollian and A. Goetzberger, Bell Syst. Tech. Jour. 46, 1055 (1967).
14. H.C. Casey, Jr., A.Y. Cho, and H. Morkoc; G.Y. Robinson, L.P. Erickson, T.E. Brady, and T.R. Ohnstein, work reported at the "Workshop on Dielectric Systems for the III-V Compounds - 1980" San Diego, Calif. May 20-21, 1980.

APPENDIX

The manuscript reproduced here will be published in the February 1, 1981 issue of Applied Physics Letters.

REACTIVITY AND INTERFACE CHEMISTRY DURING SCHOTTKY-BARRIER FORMATION:
METALS ON THIN NATIVE OXIDES OF GaAs INVESTIGATED BY XPS

Steven P. Kowalczyk, J. R. Waldrop and R. W. Grant

Rockwell International Electronics Research Center
Thousand Oaks, CA 91360

ABSTRACT

The room temperature interfacial chemical reactions of overlayers of several diverse metals (Au, Cu, Al, Mg, Cr, and Ti) with thin native oxide films (~ 10 Å) on GaAs (100) surfaces were investigated with x-ray photoelectron spectroscopy (XPS). The reactivity of these metals with the native oxides of GaAs ranged from inert to complete reduction of the oxides and is well predicted by bulk thermodynamic free energies of formation. Variations in band bending during Schottky-barrier formation were monitored by XPS. The implication of the observed interface chemistry for Schottky-barrier modeling is discussed.

Schottky-barrier junctions are the basis of a large number of compound semiconductor electronic devices, including microwave diodes, FET's, solar cells, photodetectors, and CCD's; thus, knowledge of interfacial

phenomena occurring during formation of Schottky-barrier contacts is of significant importance. A fundamental understanding of these phenomena is especially crucial as the prospect of very large scale integrated circuit technology becomes imminent. The primary experimental thrust of surface science experiments has been limited to ideal (abrupt) contacts, that is, metals deposited under ultra-high vacuum (UHV) conditions on atomically clean and crystallographically ordered semiconductor surfaces.¹⁻⁵ However, typical fabrication procedures for a Schottky-barrier device generally are such that a native oxide film is present on the semiconductor surface prior to metal deposition. For this reason modeling of practical Schottky-barrier devices generally assumes the presence of a thin (10-100 Å) interfacial insulator film between the metal and semiconductor.⁶

This letter reports x-ray photoelectron spectroscopy (XPS) investigations of Schottky-barrier formation at GaAs (100) interfaces in the presence of a thin native oxide surface layer. GaAs surfaces that had two different initial oxides were studied. The room temperature chemistry was investigated for the metals Au, Cu, Al, Mg, Cr, and Ti with an interfacial oxide layer during sequential stages of contact formation. A range of reactivity was found, from chemically inert (Cu and Au) to complete consumption of the native oxide layer (Al, Mg, Cr, and Ti). We have also used XPS to monitor the GaAs interface band bending during Schottky-barrier formation and find that the Schottky-barrier height is relatively independent of the composition of the initial thin native oxide layer.

The ability of XPS to detect the chemical state of the component atomic species in a molecule or solid is well known,⁷ including numerous applications to surface chemistry.^{8,9} The surface sensitivity of XPS is due to its ~ 25 Å sampling depth. The capability of XPS to monitor surface - or interface - potentials to high accuracy is less well known.^{10,11} Chemical information is obtained from chemical shifts of core-level binding energies. These shifts are the result of changes of valence-electron distribution. For example, the binding energy of the As 3d level in As₂O₃ is ~ 3.4 eV higher than in GaAs. For a semiconductor, band bending rigidly shifts all core-level binding energies with respect to the Fermi level, thus one can monitor the potential shift of a particular valence state to measure interface potentials. Details of potential-shift measurement and its application to interface potentials can be found in Ref. 11. The present work utilizes both capabilities.

The XPS instrumentation used for these measurements is a HP 5950A electron spectrometer with monochromatized AlK α ($h\nu = 1486.6$ eV) x-ray source and UHV modifications ($< 9 \times 10^{-11}$ torr). The sample treatment chamber included an evaporator and a quartz crystal thickness monitor for controlled metal depositions. The sample holder incorporates a resistive heater capable of producing sample temperatures up to 1000°C.

The samples were all bulk grown n-type ($\sim 5 \times 10^{16}$ cm⁻³) GaAs¹² which had been wafered and polished to give a (100) surface. Two types of GaAs (100) surfaces were prepared. Each surface was first treated with a standard sulfuric 4:1:1 (H₂SO₄, H₂O₂, H₂O) etch for approximately 1 minute, quenched in

H₂O, then inserted into the introduction chamber of the XPS spectrometer system within a few minutes. XPS analysis of relative peak heights shows that this procedure results in a ~ 10 Å thick mixed oxide consisting of both As₂O₃ and Ga₂O₃ (see Fig. 1) and an associated large surface band bending (~ 0.7 eV).¹¹ A second set of samples with a different type of oxide was prepared by heating the above mixed oxide to ~ 450°C in a vacuum of 10⁻⁹ torr for ~ 5 minutes. Such sample heating could occur during a device processing step. This heat treatment results in a surface oxide layer with about the same thickness but solely with the composition Ga₂O₃ from the reaction:



in which additional GaAs substrate is consumed.¹¹ The Ga₂O₃ covered surface is associated with a low band bending (~ 0.3 eV).^{11,13} The difference in surface potential is ~ 0.4 eV between these two surfaces. A sample with each of the oxides was prepared for deposition of the metals Au, Cu, Al, Mg, Ti, and Cr. Three regimes of deposited metal thickness were studied: (1) submonolayer, (2) ~ 1-3 monolayer and (3) thick, > 50 Å.

In Fig. 1 the XPS Ga 3d, As 3d, and Al 2p core-level peaks are shown for the initial mixed oxide surface, (a), and for four successive Al metal depositions, (b)-(e), which were made onto a mixed-oxide covered GaAs substrate. The peaks arising from the Ga and As in the GaAs substrate (labeled Ga(GaAs) and As (GaAs)) are clearly distinguishable from the chemically shifted Ga and As contributions arising from the thin oxide film

(labeled Ga(ox) and As(ox)). With the first two depositions of Al, ~ 5 Å, (b)-(c), the Al consumes As₂O₃ and becomes Al₂O₃ via the room temperature solid-state reaction:



the Ga₂O₃ is unaffected. The elemental As produced is apparently desorbed from the surface. Once the As₂O₃ is entirely consumed, additional Al, deposited in (d)-(e), reacts with the Ga₂O₃ via the reaction:



In spectrum (e) the elemental Ga produced by this reaction is apparent as a low binding-energy peak at ~ 18.3 eV; also, only when both oxides are completely reduced is metallic Al observed, as in (d) and (e). The total amount of Al deposited was ~ 40 Å. A similar sequence of depositions were made for Ti, Cr, Au, and Cu metal overlayers. Ti and Cr were more reactive than Al in that both oxides were reduced simultaneously rather than sequentially, the chemical behavior was otherwise similar. For Au and Cu deposition, on the other hand, neither oxide was chemically affected, no reduction of oxide was observed. All surfaces which had the mixed As₂O₃ and Ga₂O₃ oxides exhibited little change of surface band bending upon deposition of metal overlayers.

In Fig. 2 a series of Ga 3d peaks (a)-(e) from GaAs substrates that had the Ga₂O₃ surface are shown for a ~ 15 Å deposition, labeled (2), of Al,

Ti, Cr, Au, and Cu, respectively. In all the initial spectra, labeled (1), the pronounced shoulder on the high binding-energy side of the Ga(GaAs) main peaks is due to the Ga₂O₃ oxide film. In this series of spectra both chemical effects and a GaAs band-bending change are evident as a result of metal deposition. For example, in cases (a)-(d) a binding-energy shift of the main Ga(GaAs) peaks to ~ 0.4 eV lower binding energy is readily discernable. As discussed earlier, this type of shift corresponds to a change in band-bending potential in the GaAs. In this case, we are observing a change in interface band bending in the GaAs as a Schottky-barrier contact is being formed by the presence of a metal. For Al, Ti, and Cr, (a)-(c) this band-bending change is accompanied by Ga₂O₃ reduction and the formation of Ga alloys or compounds with the deposited metal, as evidenced by disappearance at the Ga(ox) shoulder and the appearance of the low binding-energy structure. Although not shown, Mg metal overlayers had identical behavior. Once again, Au and Cu produced no chemical reaction with the Ga₂O₃ layer, although a significant increase in GaAs band bending still occurs.

The driving force for these chemical reactions is the change in free energy of formation ΔG . The use of bulk ΔG values provides a useful rule-of-thumb⁹ for predicting all of the interfacial reactions observed in this work. However, because this predictive guide is based on bulk thermodynamic properties and does not consider interfacial contributions it should be employed with caution.

Our results have several implications for understanding the formation of Schottky-barrier contacts. Two of the important aspects of this work are

that, (1) the chemical reactivity and (2) the pinning position of the surface Fermi level can both be contactlessly monitored in the same XPS measurement during contact formation. Figure 1 shows that an initial layer of native oxide is completely consumed by reaction with certain deposited metals at room temperature to thus produce a new and different oxide (such as Al_2O_3 in Fig. 1). Figure 2 demonstrates another important concept, namely that a band-bending variation can occur during Schottky-barrier contact formation in the presence of a surface oxide. If a surface is prepared with a low surface band bending (such as the Ga_2O_3 surface of Fig. 2), the deposition of metal on the thin native oxide layer acts to shift the surface Fermi level to result in a higher band bending and thus a higher Schottky-barrier height. This new pinning position is approximately the same whether there is a chemical reaction (Ti, Cr, Al, Mg) or not (Au and Cu). Thus the distinct interfacial native oxide which is conventionally assumed in present Schottky models either does not exist or does not insulate the semiconductor from the effects of a metal overlayer. Therefore the interfacial oxide layer as is presently used in modeling Schottky-barrier heights is not appropriate for GaAs.

Since GaAs is a prototypical covalent compound semiconductor, we expect that the observed interface effects are general phenomena on compound semiconductor surfaces. We note that the metals which react with native oxides may be preferred in actual devices because they would have presumably better contact adhesive properties.

ACKNOWLEDGMENT

This work was supported in part by WPAFB Contract No. F33615-78-C-1591. We thank Dr. Peter Asbeck for informative discussion.

REFERENCES

1. R. H. Williams, V. Montgomery, and R. R. Varma, J. Phys. C 11, L735 (1978).
2. J. R. Waldrop and R. W. Grant, Appl. Phys. Lett. 34, 630 (1979).
3. P. W. Chye, I. Lindau, P. Pianetta, C. M. Garner, C. Y. Su, and W. E. Spicer, Phys. Rev. B 18, 5545 (1978).
4. K. Okuno, T. Ito, M. Iwami, and A. Hiraki, Sol. St. Comm. 34, 493 (1980).
5. L. J. Brillson, Phys. Rev. B 18, 2431 (1978).
6. See, for example, S. M. Sze, Physics of Semiconductor Devices, (Wiley-Interscience, New York 1969).
7. K. Siegbahn, C. Nordling, A. Fahlman, R. Nordberg, K. Hamrin, J. Hedman, G. Johansson, T. Bergmark, S.-E. Karlsson, I. Lindgren, and B. Lindberg, ESCA Atomic, Molecular, and Solid State Structure Studied by Means of Electron Spectroscopy, (Nova Acta Regiae Soc. Sci. Upsaliensis Ser. IV, 20, 1967).
8. C. R. Brundle, Sur. Sci. 48, 99 (1975).
9. N. Winograd, W. E. Baitinger, J. W. Amy, and J. A. Munarin, Science 184, 565 (1974).
10. E. A. Kraut, R. W. Grant, J. R. Waldrop and S. P. Kowalczyk, Phys. Rev. Lett. 44, 1620 (1980).
11. R. W. Grant, S. P. Kowalczyk, J. R. Waldrop and W. A. Hill, in Physics of MOS Insulators, ed. S. Pantelides, (American Institute of Physics, New York, to be published).
12. From Crystal Specialities, Inc.
13. A Ga_2O_3 surface layer can alternatively be prepared by heating the initial oxide to $\sim 570^\circ\text{C}$ in UHV for several minutes to produce a clean surface (which gives a characteristic LEED pattern) and subsequent oxidation by exposure to $\sim 10^4$ L O_2 at $\sim 480^\circ\text{C}$.

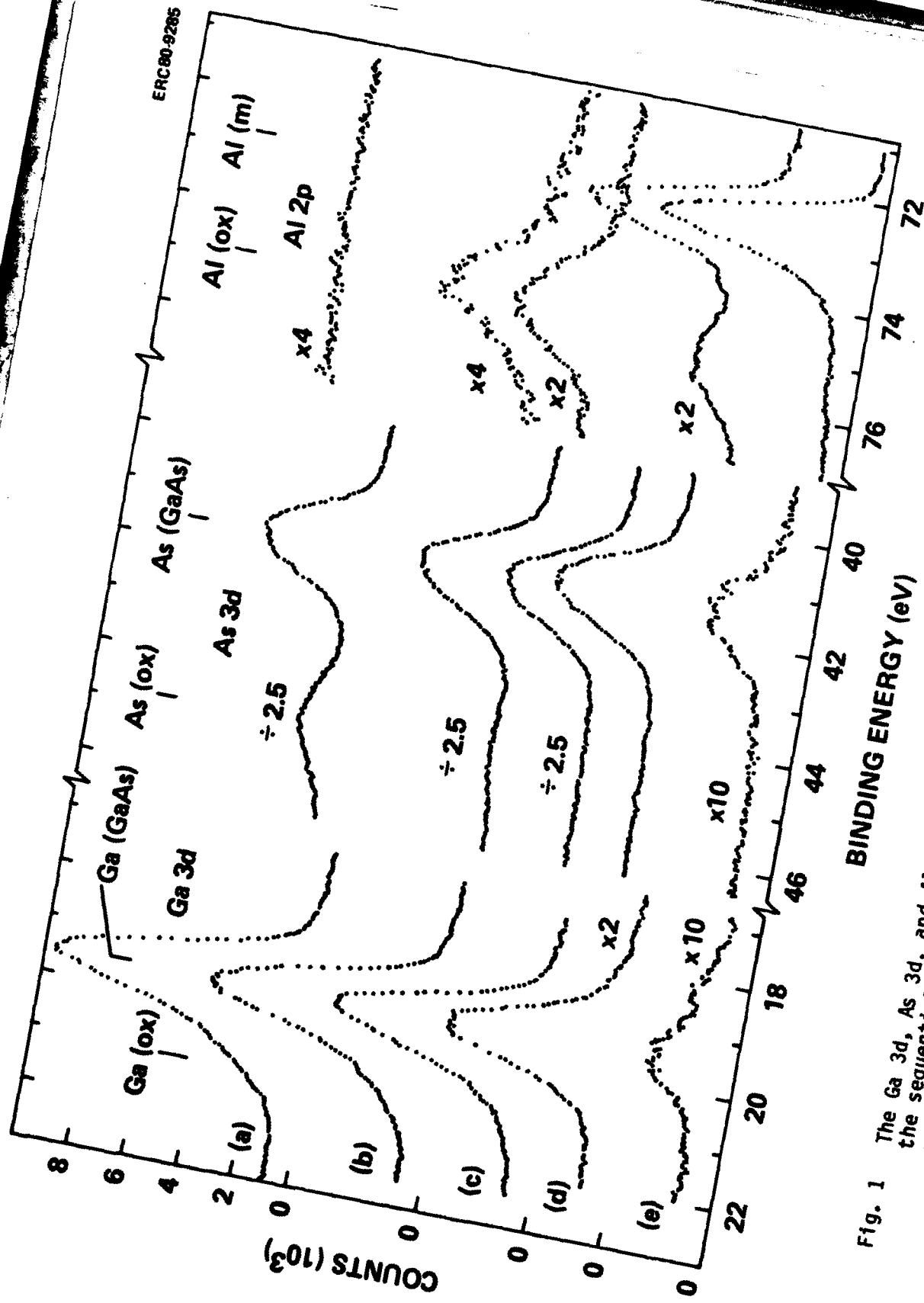


Fig. 1 The Ga 3d, As 3d, and Al 2p core-level spectra from n-GaAs (100) with the sequential treatment of (a) etch, (b) submonolayer deposit of Al, and (c-e) increasing thickness of Al deposit.

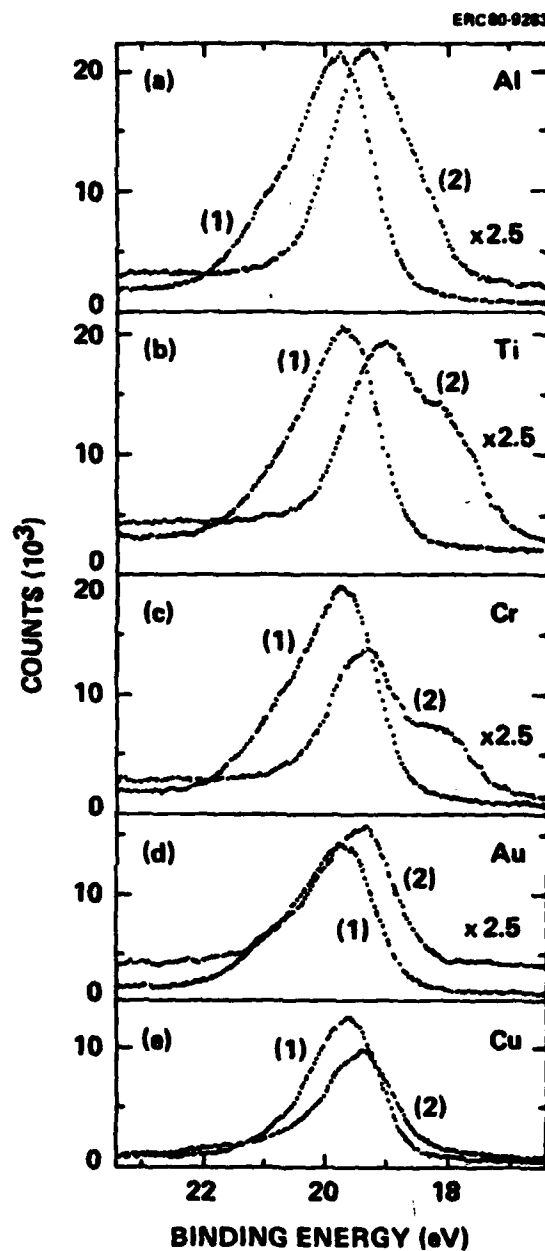


Fig. 2 The Ga 3d spectra of heat treated n-GaAs (100) with Ga₂O₃ surface layer. (1) Before metal deposition and (2) after metal deposition. Metals: (a) Al, (b) Ti, (c) Cr, (d) Au and (e) Cu.